

Energy

**F
-
S
-
S
O
F
F**

ENHANCED OIL RECOVERY BY CO₂ FOAM FLOODING

Annual Report for October 1, 1982–September 30, 1983

**May 1984
Date Published**

Work Performed Under Contract No. AC21-81MC16551

**New Mexico State University
Las Cruces, New Mexico**

**Technical Information Center
Office of Scientific and Technical Information
United States Department of Energy**



DISCLAIMER

This report was prepared as an account of work sponsored by an agency of the United States Government. Neither the United States Government nor any agency thereof, nor any of their employees, makes any warranty, express or implied, or assumes any legal liability or responsibility for the accuracy, completeness, or usefulness of any information, apparatus, product, or process disclosed, or represents that its use would not infringe privately owned rights. Reference herein to any specific commercial product, process, or service by trade name, trademark, manufacturer, or otherwise does not necessarily constitute or imply its endorsement, recommendation, or favoring by the United States Government or any agency thereof. The views and opinions of authors expressed herein do not necessarily state or reflect those of the United States Government or any agency thereof.

This report has been reproduced directly from the best available copy.

Available from the National Technical Information Service, U. S. Department of Commerce, Springfield, Virginia 22161.

Price: Printed Copy A05
Microfiche A01

Codes are used for pricing all publications. The code is determined by the number of pages in the publication. Information pertaining to the pricing codes can be found in the current issues of the following publications, which are generally available in most libraries: *Energy Research Abstracts (ERA)*; *Government Reports Announcements and Index (GRA and I)*; *Scientific and Technical Abstract Reports (STAR)*; and publication NTIS-PR-360 available from NTIS at the above address.

ENHANCED OIL RECOVERY BY CO₂ FOAM FLOODING
ANNUAL REPORT FOR
October 1, 1982 - September 30, 1983

Contributors:

Stan Holbrook
Pat Phelan
Rudi Roubicek
Joe Creed

John T. Patton
Project Manager
Department of Chemical Engineering
New Mexico State University
Las Cruces, New Mexico 88003

Albert Yost
Technical Project Officer
Department of Energy
Morgantown Energy Technology Center
P. O. Box 880
Morgantown, West Virginia 26505

Date Submitted - December 22, 1983

Work Performed for the Department of Energy
Under Contract No. DE-AC21-81MC16551

Regents of New Mexico State University
Engineering Research Center
Box 3449
Las Cruces, New Mexico 88003

Table of Contents

<u>Title</u>	<u>Page</u>
SECTION ONE.	1
INTRODUCTION	1
1.1 General.	1
1.2 Background	2
1.3 Project Summary 1979-1982.	8
SECTION TWO.	12
DYNAMIC SCREENING - THE MINI-FLOW TEST	12
2.1 Introduction	12
2.2 Dynamic Screening	12
2.3 Apparatus	13
2.4 Preparation of Surfactant Solutions.	16
2.5 Transducer Calibration	16
2.6 Experimental Run	17
2.7 Results	19
SECTION THREE.	21
MOBILITY CONTROL IN THE PRESENCE OF RESIDUAL OIL	27
3.1 Apparatus	27
3.1.1 Reservoir Model	27
3.1.2 Carbon Dioxide	29
3.1.3 Effluent Collection	29
3.1.4 Modification of Valves	30
3.2 Procedure	30
3.2.1 Preparation of Model	30
3.2.2 Start-up	31

Table of Contents (Cont'd)

<u>Title</u>	<u>Page</u>
3.2.3 Operation	32
3.2.4 Data Collection	33
3.2.5 Data Analysis	33
3.3 Results	38
3.3.1 Relative Permeabilities	38
3.3.2 CO ₂ Solubility Compensation	39
3.3.3 Estimating the Volume of Dissolved CO ₂	42
3.3.4 Corrected Equation for Injected CO ₂	42
3.3.5 Curve Fitting Equations	43
3.3.6 Most Polynomials are Unsatisfactory	46
3.3.7 Equation for Injected Gas	46
3.3.8 Equation for Produced Water	47
3.3.9 Alternative Forms	47
SECTION FOUR	49
MISCIBLE DISPLACEMENT	49
4.1 Apparatus	49
4.1.1 Reservoir Condition Flow Model	49
4.1.2 Injection Pump	52
4.2 Materials	54
4.3 Procedure	56
4.3.1 Saturation of the Model	56
4.3.2 Water and Surfactant Flood	56

Table of Contents (Cont'd)

<u>Title</u>	<u>Page</u>
4.3.3 Carbon Dioxide Tertiary Flood	57
4.3.4 Sample Analysis	57
4.4 Results	58
4.5 Conclusions	67
SECTION FIVE	69
CONCLUSIONS AND RECOMMENDATIONS	69
5.1 Research Summary	69
5.2 Process Status	70
BIBLIOGRAPHY	72
PATENTS & THESES	79
APPENDIX A	80
APPENDIX B	85

List of Tables

<u>Tables</u>	<u>Page</u>
3.1 Parameters of Reservoir Model	27
4.1 Physical Properties of n-Octance	55
4.2 Mobility Control Surfactants	55
4.3 Mobility Control Floods	59

List of Figures

<u>Figure</u>	<u>Page</u>
1.1 Carbon Dioxide Required to Produce Tertiary Oil	3
2.1 Dynamic Screening Apparatus.	14
2.2 Differential Pressure Transducer Calibration	18
2.3 Brine Mobility - Exxon LD776-52	20
2.4 Tap Water Mobility - Exxon LD776-52	22
2.5 Effect of Salinity and Temperature on Mobility Control - Exxon LD776-52	23
2.6 Static Foam Test - Sun Tech 4	25
2.7 Brine Mobility - Sun Tech 4	26
3.1 Schematic Diagram of Apparatus Used for CO ₂ Mobility Study	28
3.2 Cumulative Volume CO ₂ Injected	34
3.3 Cumulative Brine Produced.	36
3.4 Rate of CO ₂ Injection	37
3.5 Relative Permeability of Water in Presence of Oil.	40
3.6 Relative Permeability of CO ₂ in Presence of Oil	41

List of Figures

<u>Figure</u>		<u>Page</u>
3.7	Cumulative Volume CO ₂ Produced	44
3.8	Cumulative Volume Insoluble CO ₂	45
4.1	Miscible Displacement Apparatus	50
4.2	Model Entrance Construction	51
4.3	Injected Fluid Filter	53
4.4	Conventional CO ₂ Flood	61
4.5	Stepanflo 50 Mobility Controlled CO ₂ Flood	62
4.6	Pluradyne SF-27 Mobility Controlled CO ₂ Flood	64
4.7	Exxon LD776-52 Mobility Controlled CO ₂ Flood	66

ABSTRACT

Objective: Identify commercially available additives which are effective in reducing the mobility of carbon dioxide, CO_2 , thereby improving its efficiency in the recovery of tertiary oil, and which are low enough in cost to be economically attractive.

Summary: During the past year significant progress has been made in developing a commercial method of reducing the mobility of carbon dioxide in enhanced oil recovery processes. Interest in the industry is high, and several companies have agreed to underwrite a portion of funding necessary to continue the research over the next two years.

Oil recovery experiments during the past year were exclusively devoted to miscible displacement of oil by carbon dioxide; both with and without mobility control additives. The three prime chemical additives for mobility control, Stepanflo-50, Pluradyne SF-27, and Exxon LD 776-52, were used in identical displacement experiments. The results of these tests indicate that mobility control additives can enhance CO_2 miscible tertiary oil. Equally significant is the fact that the improvement in displacement efficiency correlates with the two-phase flow mobility control data obtained in the dynamic screening experiments. The corroboration of the dynamic screening results will allow a more expeditious and effective selection of additives for future field applications.

Experiments on gas mobility control, conducted in linear sand-pack models, show only a general correlation with the static foam test. The static test, which utilizes a blender to generate foam from an aqueous

surfactant solution, is useful mainly for studying the effects of pH, temperature, salinity and crude oil on the relative foamability of any given surfactant. In general, all surfactants that produce reasonable quantities of foam in the blender test also impart some degree of mobility control to gas during the two-phase flow. However, a good additive must spontaneously produce a viscous foam under flow conditions present in a petroleum reservoir.

Four basic chemical structures, listed below, appear to show most promise for gas mobility control;

1. Ethoxylated adducts of $C_8 - C_{14}$ linear alcohols
2. Sulfate esters of ethoxylated $C_9 - C_{16}$ linear alcohols
3. Low molecular weight co-polymers of ethylene oxide and propylene oxide.
4. Synthetic organic sulfonates

With the exception of the sulfonates, the above types are compatible with normal oil field brines, unaffected by the presence of crude oil and stable under conditions common in a petroleum reservoir.

The second significant result during the year involves identification of several sulfonate structures that have high potential for mobility control for carbon dioxide. Commercial sulfonate additives are available that appear optimum for reservoirs where freshwater will be used to inject the surfactant solution. They can also be considered for limited brine applications, for as temperature increases the utility of sulfonates for mobility control also increases. This is encouraging since some of the previously identified additives are chemically unstable at temperatures encountered in most petroleum reservoirs.

SECTION ONE

INTRODUCTION

1.1 General

For more than 30 years oil recovery experts have known that carbon dioxide possesses a unique ability to displace crude oil from reservoir rock. Although many gases have been tested for their crude-displacing efficacy, only carbon dioxide has the ability to reduce residual oil saturations to near zero and also to produce significant quantities of tertiary oil in models that have been previously waterflooded to the economic limit. Early studies have provided the fundamental understanding required to explain the high efficiency of carbon dioxide, and yet the depressed price of crude until recently has made most, if not all, CO₂ field applications appear to be unprofitable.

Oil displacement by gas can occur under both miscible and immiscible phase conditions. CO₂ is unique in that it can effectively displace oil in both modes, with the determining factor being largely the depth of the reservoir which controls the pressure at which the flood is conducted. All factors being equal, it is desirable to conduct the flood under miscible conditions if at all possible.

A common problem among gas-driven oil recovery processes is the severe gas channeling which occurs in the reservoir due to high gas mobility. Optimistic oil recoveries obtained in laboratory flow tests using small diameter, linear models have never been achieved in the field.

Both miscible and immiscible drive processes suffer because gas channeling causes most of the oil reservoir to be bypassed and the oil left behind.

Because of the high potential for miscible drives using enriched gas mixtures, considerable study was undertaken in the late 1950's on techniques to mitigate gas channeling. A few visionary investigators considered the use of foams as a possible solution to the problem. The earliest reported work was conducted by Bond and Holbrook whose 1958 patent describes the use of foams in gas-drive processes [106]. Because of the high cost of carbon dioxide relative to crude oil during this period, carbon dioxide processes were ignored. The use of foams in conjunction with carbon dioxide was not contemplated until much later when rising crude prices coupled with an increase in value of hydrocarbon gases revived interest in the carbon dioxide displacement technique.

1.2 Background

Before embarking on the experimental phase of this research project, an extensive literature review was undertaken to evaluate the current state-of-the-art and to identify techniques, both good and bad, that had been investigated in the past. The resulting bibliography is included in this report.

The majority of both field and laboratory results which appear in the literature have been summarized by Patton [56] and are presented in Figure 1.1. These data have been normalized to a constant CO_2 injection equal to 0.2 pore volumes. It is apparent that above an oil viscosity of 2 centipoises the experiments indicate an almost constant displacement efficiency for carbon dioxide processes.

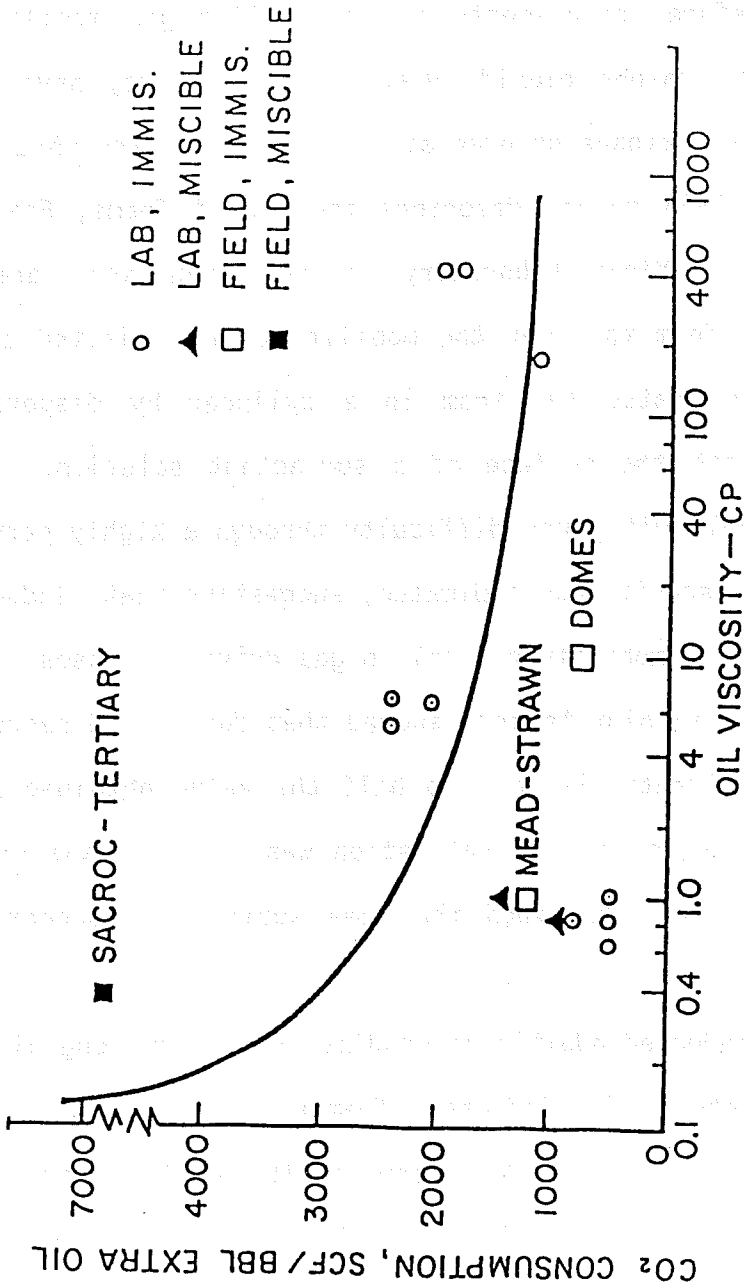


FIG 1.1: Carbon Dioxide Required to Produce Tertiary Oil

The earliest work relative to the problem of lowering the mobility of carbon dioxide does not involve carbon dioxide at all. Carbon dioxide exists as a gas or super critical phase under most reservoir conditions; therefore, experiments on controlling gas mobility are usually applicable to carbon dioxide even though they may have been conducted with nitrogen, methane or even air. Concurrent with Bond and Holbrook's work, whose 1958 patent describes the use of foams, Fried, working at the Bureau of Mines Laboratory in San Francisco, demonstrated the potential of foam to lower the mobility of an injected gas phase [27].

Fried generated the foam in a cylinder by dispersing fine air bubbles beneath the surface of a surfactant solution. This foam was flowed but only with much difficulty through a highly permeable matrix. A high foam-viscosity was indicated, suggesting that, indeed, foam might be the answer to mobility control in gas drive processes. Oil displacement tests in an Aloxite core showed that foam could reduce the saturation of a 350 centipoise oil to half the value obtained by waterflooding. The reduction in oil saturation was purely a viscous flow effect as the waterflood contained the same surfactant concentration as the foam.

Fried conducted additional studies in a 30 cm long glass-bead pack, 0.78 cm diameter, that indicated foam might be too good as a mobility control agent. Although the permeability of the pack was about 12 darcys, the foam was too viscous to flow even at a pressure gradient of 15 psi/ft. Microscopic examination of the linear model indicated that the injected foam coalesced, and was regenerated as the gas and water moved through the tiny pores. The regenerated foam had smaller bubbles and had presumably, a much higher viscosity. After a substantial amount

of regenerated foam had been formed, the mobility was lowered to the point that steady-state flow could not be maintained. From these experiments Fried concluded that a highly stable foam would not be desirable in an oil recovery process.

Fried's work was followed by some excellent work by Bond, Bernard and Holm [5,7,10,38] whose experimental technique involved in-situ foam generation promoted by injecting alternate slugs of surfactant solution and gas. Especially pertinent is their patent related to the use of foam for mobility control in CO₂ processes [104].

Laboratory work was encouraging enough that Union Oil Company conducted a field test in the Siggins Field, Illinois [35]. Foam generation by alternate slug-injection as well as simultaneous gas-solution injection was tested. This test indicated that the foaming agent, a modified ammonium lauryl sulfate, at concentrations below 1%, did not produce an effective foam. Above 1%, reduced gas mobility was obtained; however, at least 0.06 PV of surfactant solution had to be injected to achieve lasting mobility control. Inasmuch as the tests were conducted sequentially with the higher concentrations injected last, it is possible that the required amount of surfactant may be understated. Possibly a tenth-of-a-pore-volume bank might be more realistic for lasting mobility control. The results also indicated that adsorption may reduce the effectiveness of a surfactant. Future tests might benefit by selection of agents which are less strongly adsorbed than lauryl sulfate.

Work from the mid-60's to the early 70's proceeded sporadically due to the low incentive provided by the depressed price of crude oil. Interest was maintained largely by the impressive attempt by Chevron to commercialize the CO₂ process at Sacroc. Although this project suffered

from the same gas channeling noted earlier, CO₂ was effective in displacing commercial quantities of oil. Sacroc is regarded as the pioneering success for CO₂ processes.

The recent publications are especially pertinent. The first by Kanda and Schechter [43], corroborated much of the earlier work by Union, Amoco and Professor Marsden at Stanford University, and served to highlight the mechanisms and pertinent variables relative to foam mobility control. Specifically they concluded that:

1. Displacement efficiency of foams is inversely related to the surface tension between the gas and liquid constituents.
2. High surface-viscosities are beneficial in improving displacement efficiency.
3. Permeability reduction, interpreted as meaning mobility control, is achieved more by films forming across the pore openings than by the physical movement of foam past mineral surfaces in the pore matrix.
4. By far the most important variable is the ability of the surfactant solution to wet the mineral surfaces in the matrix.

This last item has not been widely recognized and bears additional discussion. Experiments were conducted in sand packs conditioned to provide varying degrees of water-wetness. When the matrix was oil wet, drastic reduction in displacement efficiency occurred. The mere presence of oil had little influence on mobility control; however, when the oil was initially allowed to contact the dry, sand surfaces, it reduced water-wetness and subsequent displacement efficiency. A similar result was obtained when the sand grain surfaces were treated with an oil-wetting silicone prior to being saturated with water.

Interpretation of these results in terms of reservoir performance is hazardous because of two factors. First, the displacement tests were

conducted in a sand pack having a permeability of 27 darcys and a porosity of 42%. The pore dimensions in these media are unrealistically high and may have caused anomalous experimental results. The second factor involves the very low concentration of surfactants employed. Kanda & Schechter believe surfactant concentrations above the critical micelle concentrations are of no advantage and, hence, used very dilute solutions, about 10^{-3} M [44]. Tests by Holm et al. [36], indicate that there is a concentration effect and that this variable should be investigated in the future.

A more recent theoretical study by Slattery [72] suggests that displacement efficiency is proportional to surface tension. It then follows that the optimum foaming agent is one which lowers surface tension only the minimum required for spontaneous foaming to occur in the reservoir. Slattery's predictions are supported in part by experimental observations reported by other authors [35,43,47]. It is possible that deviations from theory are the result of grossly different pore dimensions utilized by the different investigators. Slattery's work also supports the dominant effect wettability exerts on the control of CO_2 mobility by foam.

The recent work by Bernard, et al. [82] provides the most definitive experimental data supporting the use of surfactants to control the mobility of CO_2 . This study included linear flow tests conducted in sandstone and carbonate cores both with and without oil present in the matrix. Tests were conducted using supercritical CO_2 at pressures ranging from 1000-3050 psig. Many surfactants were screened and one, Alipal CD-128 was judged superior for lowering the mobility of CO_2 . Alipal CD-128 is an anionic surfactant synthesized by ethoxylating a linear alcohol and reacting the subsequent product with SO_3 to obtain

an anionic surfactant. Tests were made utilizing this surfactant at two concentrations, 0.1% wt and 1.0% wt. These concentrations are based on the commercially available form of the surfactant, which is listed as being only 58% active.

Although the mobility reduction was evident in both carbonate and sandstone cores the effect in the sandstone was more dramatic. CO₂ mobility was reduced 99% in sandstone as opposed to only 85% in the carbonate core. Similar tests were repeated in carbonate cores after an oil saturation had been established in the pore spaces. As was the case when no oil was present, mobility of CO₂ was reduced; however, this time it was in excess of 95% over a large number of individual experiments. The fact that mobility was reduced even more in the presence of oil strongly supports the feasibility of the concept.

With oil present, tests were run at two surfactant concentrations, 0.1% and 1.0%. In every case the more concentrated solution achieved much greater mobility lowering, 10 fold or more, than in the 0.1% experiments. This is somewhat surprising since the c.m.c. for Alipal CD-128 is thought to be well below 0.1%. In all of the experiments the lower concentration was tested first and the results may be reflecting the adsorption of the surfactant on the mineral surfaces and the residual oil droplets.

1.3 Project Summary 1979-1982

Static foam tests, performed on 113 commercial surfactant samples, have identified some optimum chemical structures for mobility control additives. A unique dynamic screening process involving a mini-flow test has been developed to quickly identify new more-promising additives. The

potential of additives, identified in these tests, have been confirmed in linear, two-phase flow tests in tight, unconsolidated sand packs.

Linear flow experiments on gas mobility control, conducted in the sand-pack models, show only a general correlation with the static foam test. The static test, which utilizes a blender to generate foam from an aqueous surfactant solution, is useful mainly for studying the effects of pH, temperature, salinity and crude oil on the relative foamability of any given surfactant. In general, all surfactants that produce reasonable quantities of foam in the blender test also impart some degree of mobility control to gas during two-phase flow. The best mobility control additives however, are only modest foam volume producers. In addition, the best additives spontaneously produce a viscous foam under flow conditions present in a petroleum reservoir.

Results of the dynamic screening tests correlate very well with both the linear mobility as well as oil displacement experiments. There is considerable evidence that the three basic chemical structures listed below appear to show most promise for gas mobility control;

1. Ethoxylated adducts of $C_8 - C_{14}$ linear alcohols
2. Sulfate esters of ethoxylated $C_9 - C_{16}$ linear alcohols
3. Low molecular weight co-polymers of ethylene oxide and propylene oxide.

Each of the above types are compatible with normal oil field brines, unaffected by the presence of crude oil and stable under conditions common in a petroleum reservoir. Additive stability is of real concern. Limited experimentation suggests that only the sulfate esters might degrade at an unacceptable rate. This could limit their application to lower temperature reservoirs. No degradation was noted for

structures 1 and 3 in aging tests lasting 2 weeks at 125°F. Some synergism exists between additives. Amine oxides and amides improve foam stability for many anionic surfactants but at the expense of some mobility control.

To elucidate the mobility control mechanism, a capillary viscometer was constructed to measure the rheological properties of foam containing the most promising additives. Foam for viscosity measurements was generated in a porous matrix representative of pore dimensions found in petroleum reservoirs. Foam was also generated in a shear-type mixer and then tested in the viscometer. Results are qualitatively similar to the matrix generated foam.

Data collected at different shear rates show foam is mildly pseudoplastic in nature and several orders of magnitude more viscous, (i.e. 10-100 cp) than its gas or liquid fraction. Of a special significance is the fact that foam viscosity has been shown to be an inverse function of foam density over a wide range of compositions. This fact is very advantageous in oil displacement processes. In areas where gas fingering is pronounced, foam viscosity would be increased with gas saturation and, thereby, tend to mitigate further gas channeling.

This high-viscosity effect of the foam suggests that the displacement of oil by foam, envisioned by early investigators, may not be the dominant mechanism under actual reservoir conditions. Alternately, the spontaneous generation of a viscous foam phase may serve to artificially reduce the flowing-gas saturation and thus provide a dramatic lowering of gas mobility due largely to a relative permeability effect. This mechanism could be especially important in the WAG process utilizing carbon dioxide or enriched gas mixtures for the displacement of oil in both miscible and immiscible processes.

The efficacy of CO₂ mobility control in enhancing oil recovery was demonstrated experimentally. Flow tests were conducted with a viscous oil under immiscible displacement conditions. Mobility control increased recovery by 40% over a CO₂ enhanced waterflood and 93% over a conventional waterflood plus primary production. No adverse effects, such as emulsion formation, due to mobility control additives were noted. Mass transfer of CO₂ from the foam to the oil did not appear to be impeded. In fact, the mobility control experiment was performed without the severe gas and liquid slugging which characterized conventional CO₂ laboratory floods.

Information on the various facets of the project have been the subject of three technical papers. Two papers were presented at the 1981 SPE/DOE Symposium held in Tulsa, Oklahoma and a third at the 182nd ACS National meeting held in New York City, August 1981. In addition, many informal discussions have been held with industry and government personnel who have visited the laboratory facilities in Las Cruces. During the course of the project, 8 graduate and 43 undergraduate students have assisted in various phases of the research, 6 M.S. degrees in Chemical Engineering have been awarded and 14 of the undergraduates accepted positions in the oil industry following their graduation. The specialized training in EOR technology that the students receive is of significant value in addition to the project's technical progress and accomplishments.

DYNAMIC SCREENING - THE MINI-FLOW TEST2.1 Introduction

New additives are screened by conducting two tests that provide a rapid initial evaluation of given additives potential for reducing the mobility of carbon dioxide in a reservoir environment. The initial test involves generation of foam under high shear and measuring the key parameters, quality of foam produced and the stability of this foam with the respect to time. The procedure involved in these tests as well as the static screening results on 92 additives have been reported previously [88].

To provide a more critical evaluation for those additives showing a high potential in the static foam test, a mini-flow test involving the two-phase flow of air and brine was developed. During the past year, the dynamic screening experiments were expanded to provide an insight into the effect of salinity and temperature on ability control. Specifically, research was concentrated on organic sulfonates whose performance in brine was well below average due to their incompatibility with divalent cations. These type of surfactants are used extensively in chemical flooding and have been field tested for use in controlling the mobility of steam in thermal operations.

2.2 Dynamic Screening

The mini-flow test was developed to provide rapid evaluation of the effect of surfactant additives on gas-liquid flow in an oil reservoir.

Analysis of the ability of various surfactants to lower the mobility of gas flowing in a porous medium was accomplished by calculating the mobility ratio of gas-to-liquid during sequential flow at equal rates. Mobility was chosen as the basis for analysis to avoid any controversy that may exist concerning the mechanism of the flow of foam in porous media. Since mobility of any fluid is known to be inversely proportional to its ΔP , mobility ratio is easily calculated by the following formula

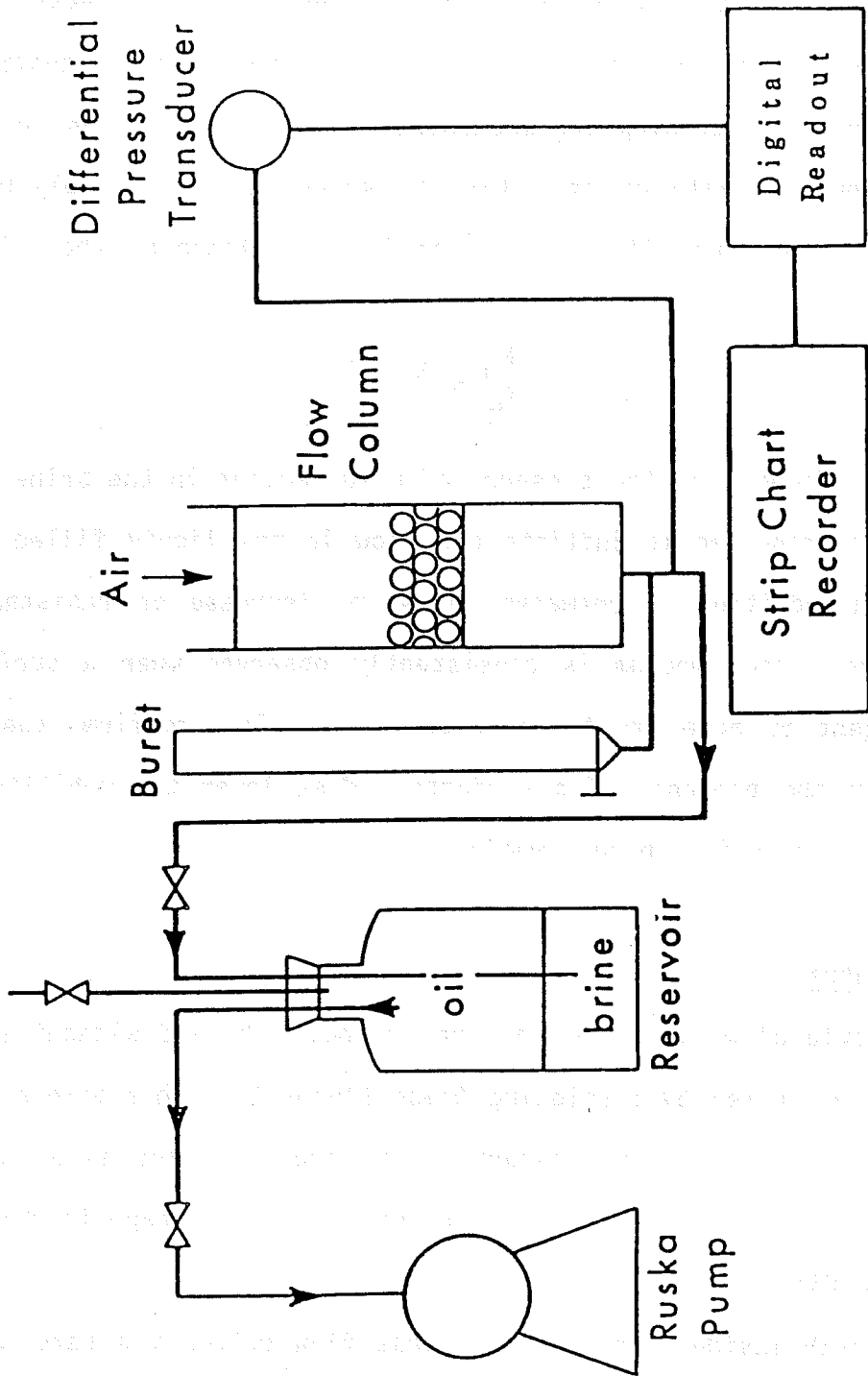
$$\frac{M_g}{M_l} = \frac{q_g \Delta P_l}{q_l \Delta P_g}$$

It was found that the presence of a surfactant in the brine lowers the pressure required to initiate gas flow in the liquid filled porous medium. In addition, a permanent pressure increase or resistance to flow in the porous medium is consistently observed when a surfactant foaming agent is added to the aqueous phase. This confirms the hypothesis that the presence of a surfactant does lower the mobility of a flowing gas stream in a porous medium.

2.3 Apparatus

The ratio of mobility for gas and brine, with and without surfactants, was evaluated by displacing these fluids through a porous medium at a constant flow rate and recording the pressure drop as a function of time. A schematic of the apparatus used to obtain experimental data is shown in Figure 2.1.

A $1\frac{1}{4}$ inch inside diameter plexiglass flow column was used to hold the porous media. The flow column consisted of two pieces. The pieces were machined so that they could be interconnected. A 100 Tyler mesh copper screen, which served as a support for porous media, was placed in



Dynamic Screening Apparatus

FIG 2.1

the collar of the bottom section and the sleeve of the upper section held the screen in place. A rubber O-ring was used to keep the flow column from leaking where the two pieces were connected. Two advantages arise from this type of flow column. First, the support screen can be easily removed for cleaning. Second, by filling the bottom section of the flow column with liquid before putting the screen in place, trapped air under the screen can be avoided.

The sand pack used in experimental runs is packed in 3 stages or layers. The bottom layer consists of 10 gm of -70 + 100 Tyler mesh glass beads. A second layer containing 10 gm of -100 + 140 glass beads is then added. A final top layer consists of 105 gm of -140 + 200 Tyler mesh glass beads. Replicate columns, so constructed, were used to test all of the surfactants and brine during the year. The total height of the glass bead pack was 4.4. inches.

Solution is withdrawn from the bottom of the flow column with a Ruska proportioning pump. It is capable of pumping or withdrawing fluid at a rate of 10 to 1200 cc/hr. by the action of a 500 cc piston type transfer cylinder powered by a $\frac{1}{4}$ horsepower drive motor.

Pressure readings were taken with a Gould-Statham, model number PM6TC, + 10 psi differential pressure transducer connected to a Gould-Statham, model number SC1012, digital readout. the transducer readout is a self-contained portable unit which provides DC excitation for a bridge transducer, digitizes the transducer output, and also provides a high-level DC output to drive a recorder or analog meter. For this work, a linear Instruments Corporation, model number 385, strip chart recorder was connected to the digital readout to observe the pressure profile as an experiment was being run. The digital readout also provides a wide

range of sensitivity and zero balance adjustments to accommodate transducer sensitivities from 1 millivolt/volt to 80 millivolts/volt and an unbalance of +115% full scale. The transducer used in this work had a sensitivity of 4 millivolts/volt and the offset was set at +20% of full-scale.

All connecting lines of the apparatus consisted of $\frac{1}{4}$ inch polyethylene tubing. All connections were made with brass fittings.

2.4 Preparation of Surfactant Solutions

The brine used to prepare solutions consisted of 3% sodium chloride and 100 ppm Ca^{++} mixed in deionized water prepared by reverse osmosis. Most of the surfactant solutions were prepared by weighing out 10 grams of surfactant and diluting with 200 milliliters of brine in a beaker. The surfactant solution was then transferred to a two liter volumetric flask and the flask filled with brine to the mark, allowing any foam to decay before adjusting the final volume.

The solutions were mixed with a magnetic stirrer while the pH was adjusted to 2.5 to simulate the acidic conditions which would be present when the solutions contact carbon dioxide in an oil reservoir. Surfactant solutions were prepared the day before use and discarded after three days.

2.5 Transducer Calibration

To begin an experimental run the differential pressure transducer was calibrated. The reference pressure for the transducer was atmospheric pressure. The calibration was done against a Wallace and Tiernan differential pressure gauge, model number FAXA 141561. The digital

readout was arbitrarily set to indicate 0.000 at a pressure of 0 psid and 0.100 at a pressure of 0.5 psid. A typical calibration curve is shown for the transducer from 0 to 10 psid in Figure 2.2.

2.6 Experimental Run

An experimental run consists of first filling all connecting lines of the system with brine or surfactant solution. The bottom section of the flow column is then filled with liquid, the copper support screen laid in place and the balance of the flow column filled to a calibration mark. This mark is the liquid level at which the transducer is adjusted to indicate 0 psid. The glass beads are then slowly poured into the flow column in successive layers and the liquid level re-established at the calibration mark by withdrawing liquid into the buret. By noting the liquid removed from the column to re-establish the level at the calibration mark, the solid volume of the bead pack could be determined. Subtracting this volume from that calculated from the height and diameter of the column allows one to determine the porosity of the bead pack.

After the volume and porosity of the bead pack are determined, the Ruska pump is turned on, the timer started and the pressure drop data recorded. The Ruska pump is set to withdraw fluid from the flow column at a rate of approximately .025 cc per second. The liquid flow rate was checked during a run by reading the volume of liquid withdrawn on the Ruska pump vernier scale and noting the time elapsed. These data were used to check the computer-calculated flow rate used in determining mobility ratios. The flow rate varied a maximum of two percent during an experimental run. A run was terminated after the liquid had been

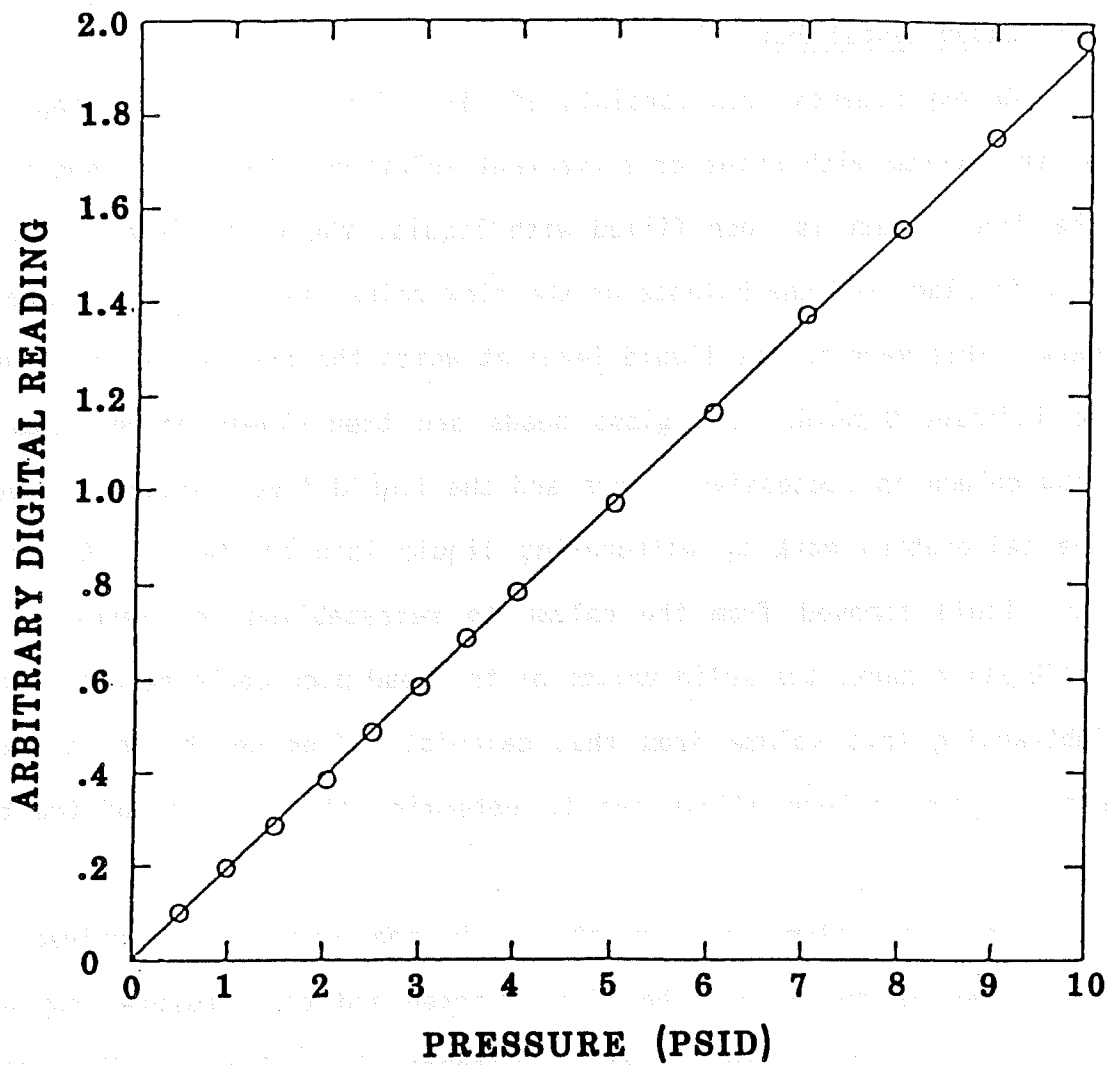


FIG 2.2: DIFFERENTIAL PRESSURE TRANSDUCER CALIBRATION

withdrawn several inches below the bead pack. At the conclusion of an experimental run, the brine or surfactant is drained from the apparatus and the flow column is disassembled and thoroughly rinsed with deionized water prepared by reverse osmosis. All connecting lines are also rinsed with deionized water to remove all traces of brine or surfactant. Prior to the beginning of a new experimental run, the apparatus is rinsed with the fluid to be tested.

2.7 Results

Prior to 1983, all organic sulfonate type additives, submitted for testing, were found to be unacceptable due to their low solubility in brine containing polyvalent cations. During the past year, several specially tailored sulfonate additives were submitted for testing. Of this group, one sample was found to possess interestingly superior performance. Although the foam produced in the static screening test with LD 776-52 would place it toward the lower end of the scale, its performance was significantly better than all other sulfonates. For this reason LD 776-52 was evaluated in the dynamic screening test. In spite of the low foam produced in the static tests, LD 776-52 provided mobility control to gas flow comparable to some of the better additives previously identified. LD 776-52 is a synthetic sulfonate as opposed to natural products obtained by sulfonation of carefully selected petroleum fractions.

The complete mobility ratio curve for LD 776-52 in the standard brine is shown in Figure 2.3. Plotted on the same graph is the mobility ratio trace obtained with the well recognized mobility control additive, Alipal CD-128. Both additives reduced mobility ratio to a value well

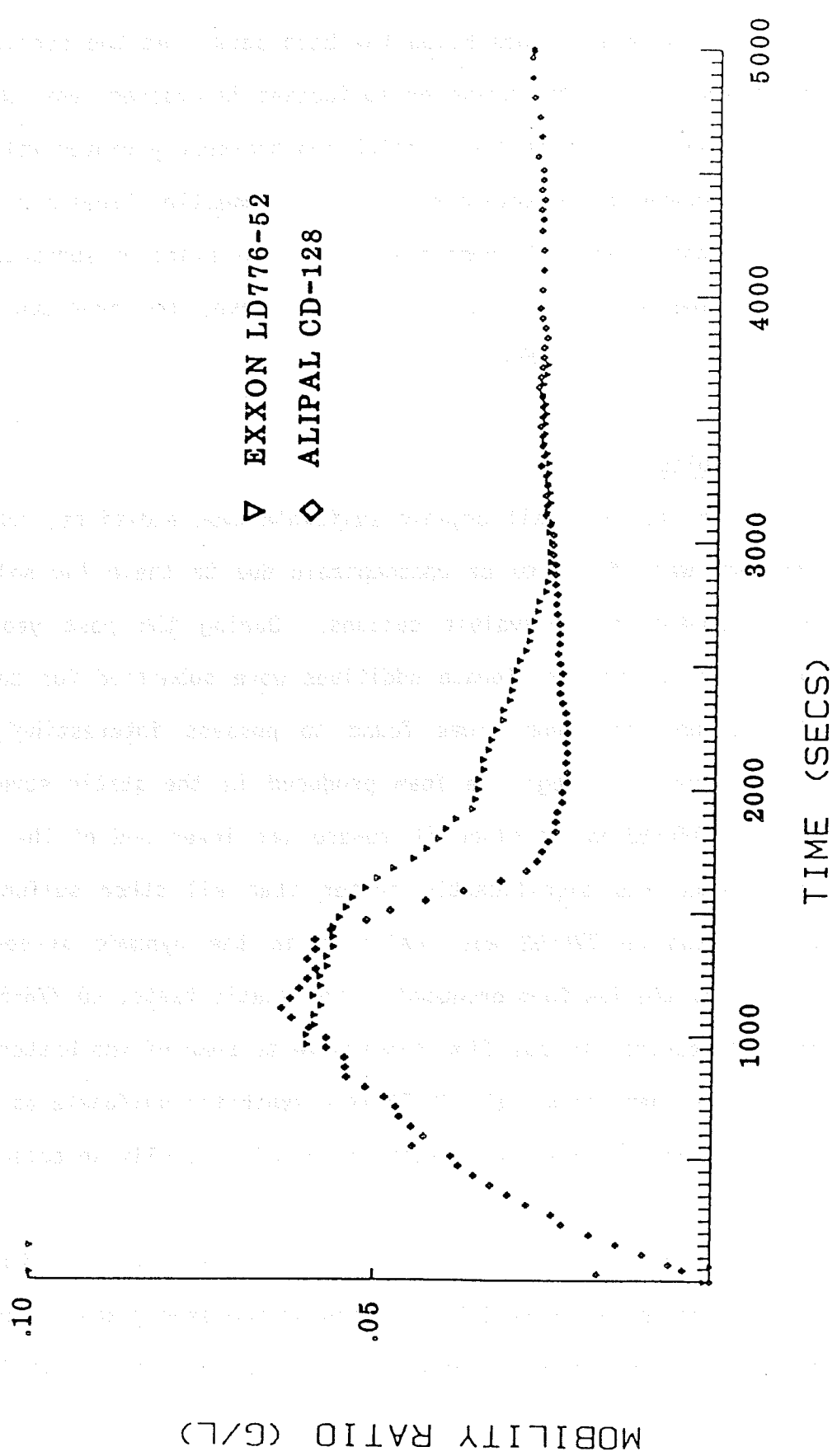
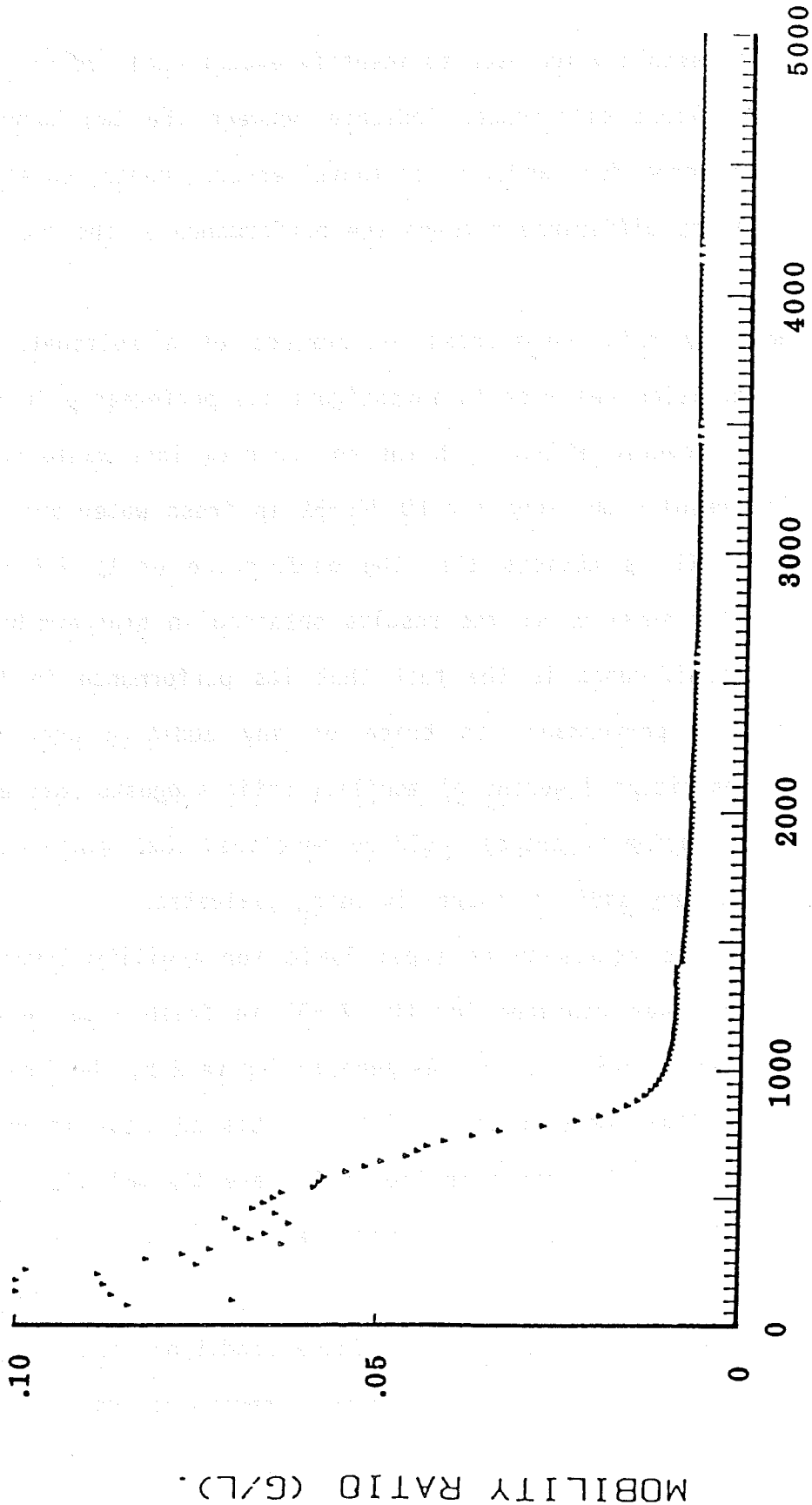


FIG 2.3: Brine Mobility - Exxon LD776-52

below 0.05, a threshold value used to identify exceptional additive performance. The slight differences indicate between the two curves is in the range expected for random experimental error. Hence, no statistically significant difference between the performance of the two additives is inferred.

Encouraged by this unsuspected performance of a sulfonate type additive, the decision was made to investigate its performance in fresh water where the adverse effect of brine and calcium ions would not be a factor. The results obtained for LD 776-52 in fresh water are shown in Figure 2.4. It is obvious that the performance of LD 776-52 in fresh water is far superior to the results obtained in standard brine. Of even more significance is the fact that its performance in fresh water exceeds the performance in brine of any additive previously tested. The significant lowering of mobility ratio suggests that additives having more brine tolerance could be developed that would exceed the performance of any additive currently being evaluated.

In an effort to determine an upper limit for mobility lowering, the mini-flow test was repeated for LD 776-52 in fresh water but an elevated temperature, 170°F (77°C). As seen in Figure 2.5, the increase in temperature further improved the ability of this additive to reduce the mobility of gas. Also shown in Figure 2.5 are the mobility ratio curves obtained in brine and in fresh water at room temperature. The trend of the curves favor the performance of sulfonates in high temperature reservoirs where salinity is low. These conditions usually preclude the use of the popular sulfate ester structures due to their tendency to hydrolyze in high temperature reservoirs. Ethoxylated



MOBILITY RATIO (G/L).

TIME (SECS).

FIG 2.4: TAP WATER MOBILITY - EXXON LD776-52

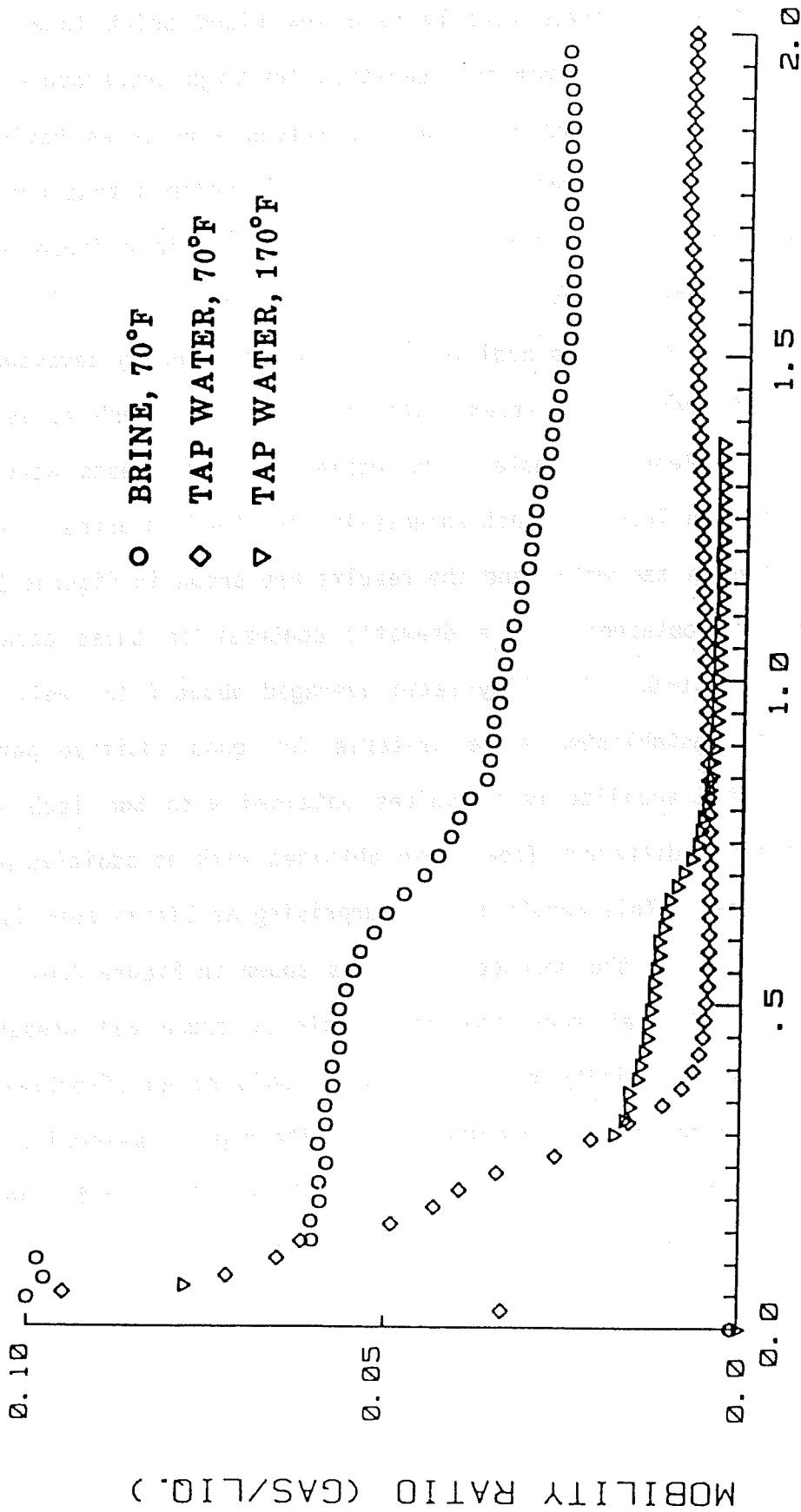


FIG 2.5: Effect of Salinity and Temperature on Mobility
 Control - Exxon LD776-52

alcohol type additives usually have low cloud point temperatures and could be eliminated from consideration for high temperature reservoirs for this reason. Even for those additives structures having no such restriction, it is doubtful one would be developed that would be more effective in reducing the mobility of the gas in a fresh water, high temperature environment.

A second sulfonate additive tested was previously developed for use in mobility control of steam. This material, Sun Tech 4, is a C₁₅-C₁₇ alkylated xylene sulfonate. The normal mobility tests were not conducted as Sun Tech 4 is not soluble in the standard brine. Instead, it was tested in tap water and the results are shown in Figures 2.6 - 2.7. The results obtained were a dramatic contrast to those obtained with Exxon's LD 776-52. Mobility ratio averaged about 0.15, well above the 0.05 level established as a criteria for good additive performance. In fact, the mobility ratio values obtained with Sun Tech 4 are not significantly different from those obtained with no additive present in aqueous phase. This result is not surprising as little foam is produced by Sun Tech 4 in the absence of oil as shown in Figure 2.6. Since all data were taken at room temperature without crude oil present, there remains the possibility that Sun Tech 4 could be an effective additive provided the reservoir temperature was quite high. Obviously, this case exists in steam floods and undoubtedly explains its superior performance in laboratory experiments relative to the mobility of steam in a porous medium.

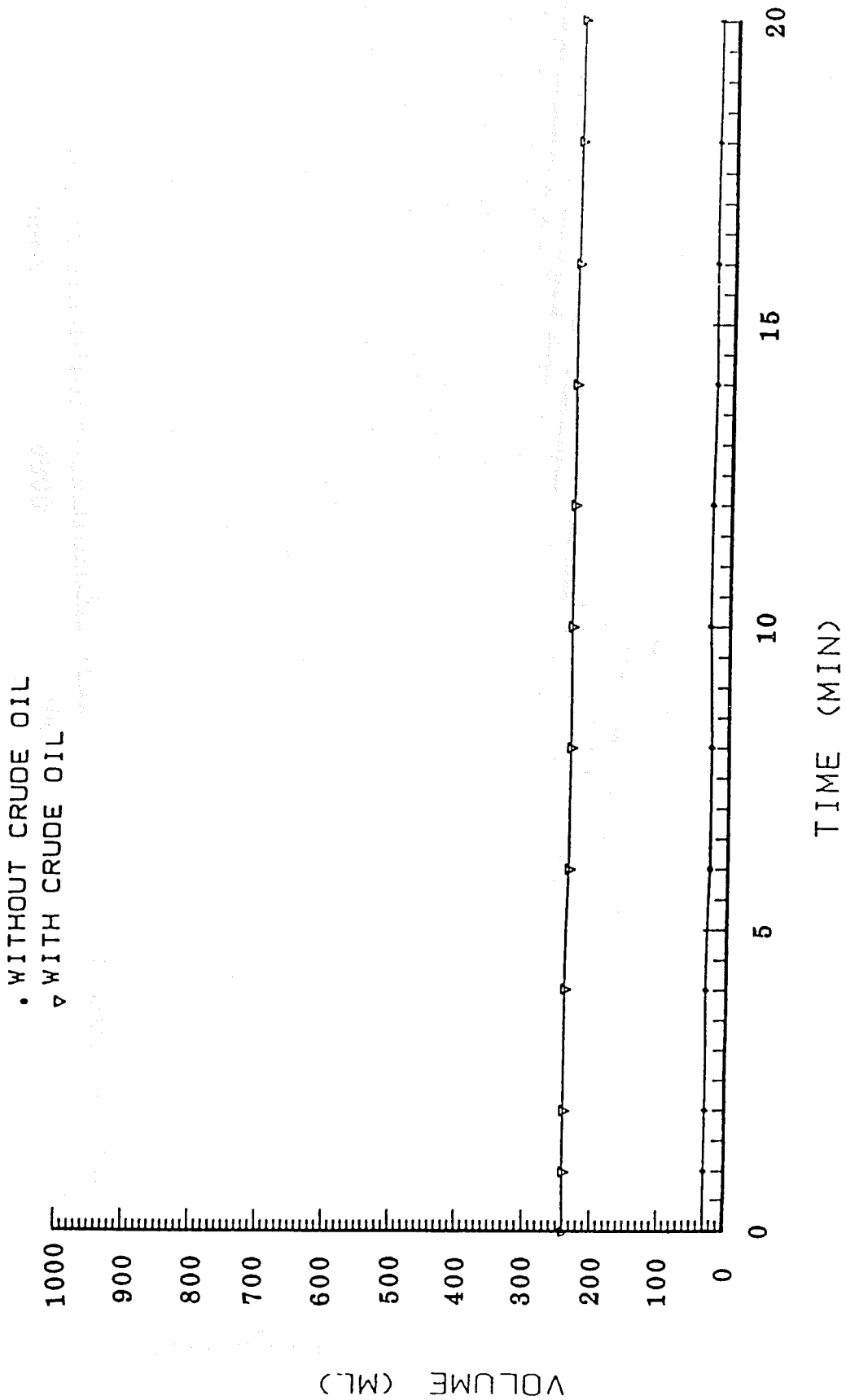
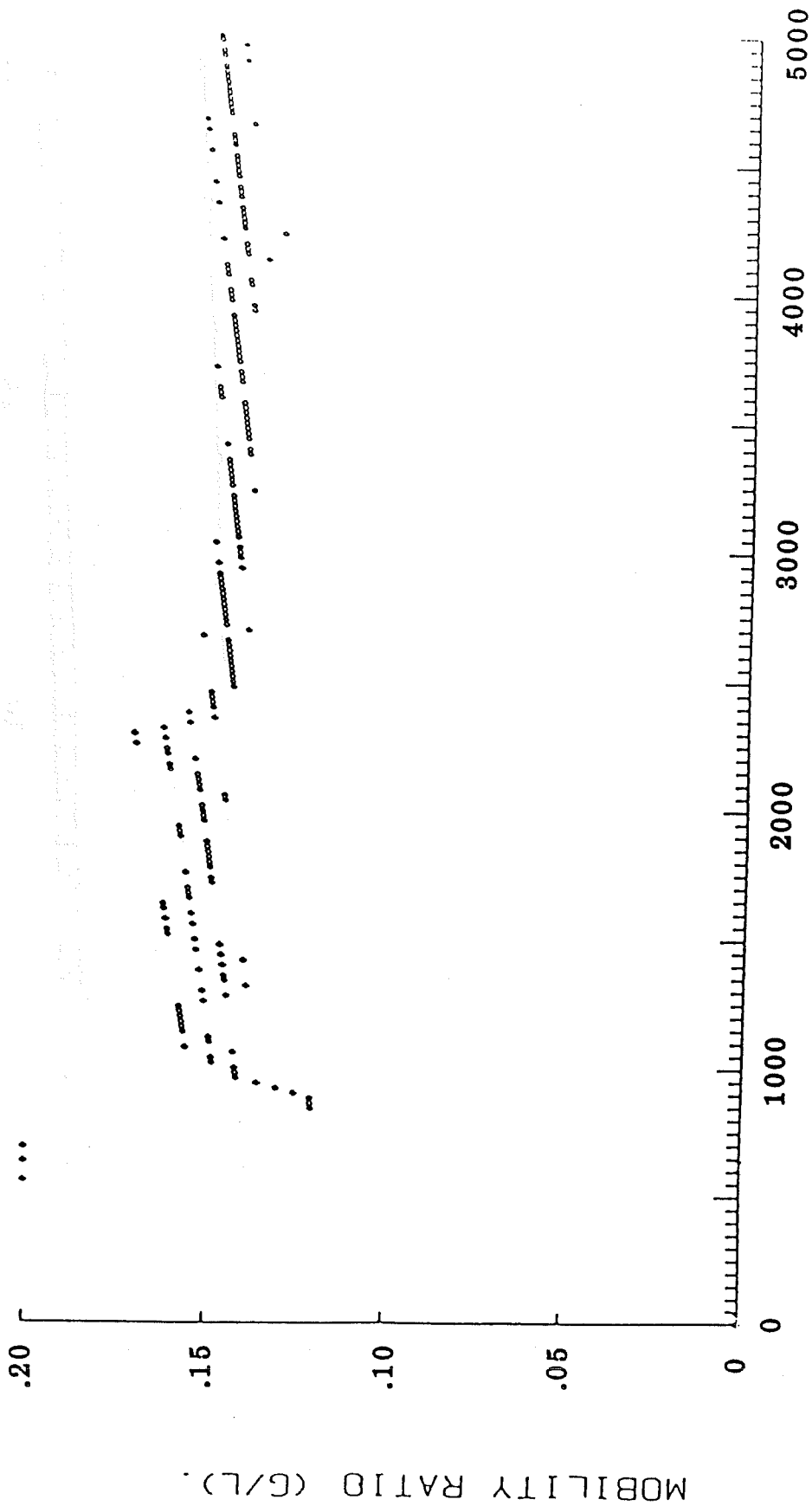


FIG 2.6: STATIC FOAM TEST - SUN TECH 4



TIME (SECS).

FIG 2.7: BRINE MOBILITY - SUN TECH 4

SECTION THREE

MOBILITY CONTROL IN THE PRESENCE OF RESIDUAL OIL

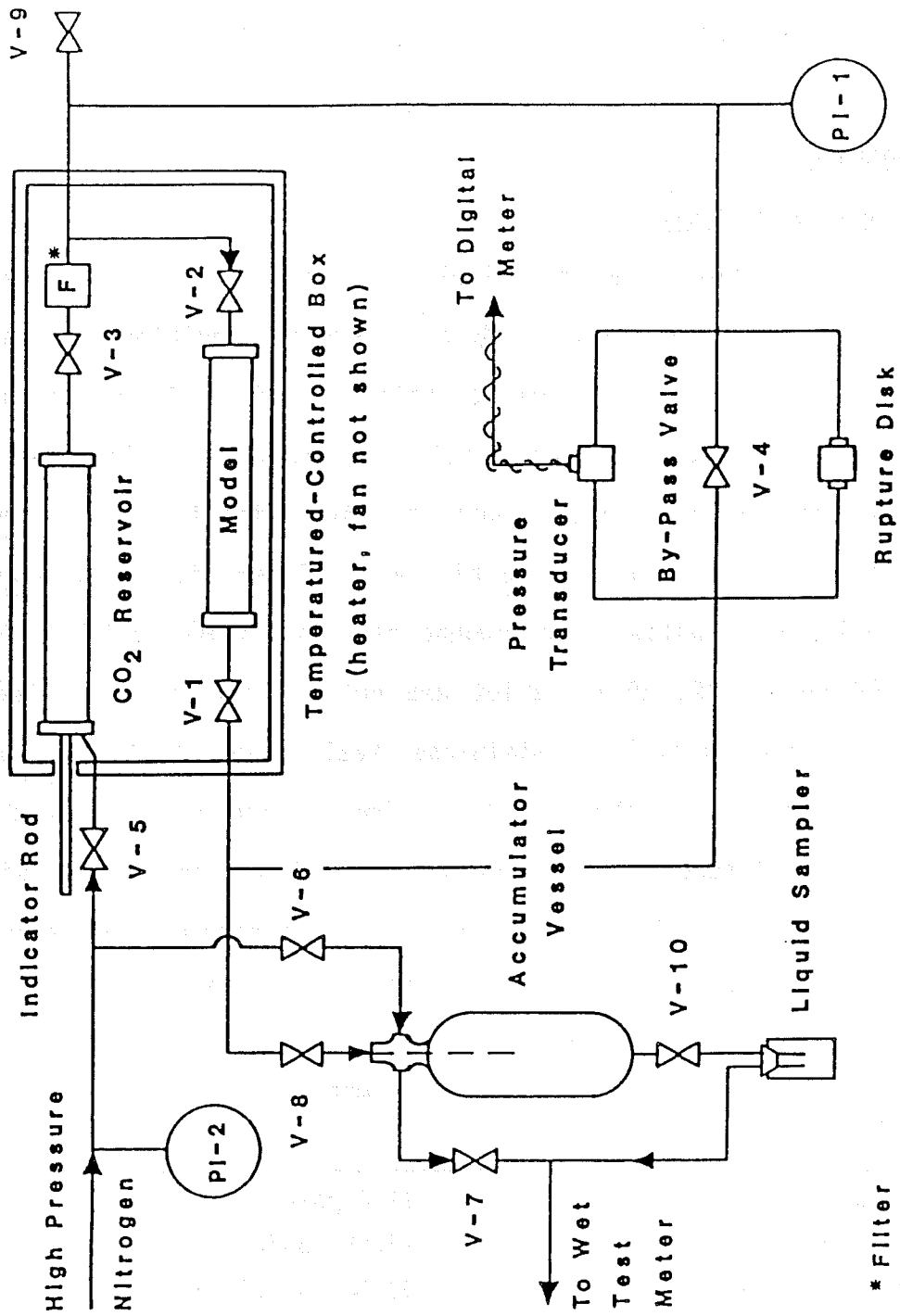
3.1 Apparatus

3.1.1. Reservoir Model

An unconsolidated sand pack simulating a portion of an oil reservoir was used for the CO₂ mobility study at reservoir conditions. As depicted in Figure 3.1, the pack was contained within a 1½ in. diameter, seamless, Sch. 40 stainless-steel (316L) pipe, 24½ in. long (62 cm). Welded to the ends of the pipe were two 316L stainless steel 900-lb, slip-on flanges. The ends of the pipe were closed with blind flanges, between which were bolted spiral-wound asbestos-filled gaskets (Flexitallic, CG 9-1500 API 601). Inlet and outlet ports were drilled and tapped for connection to ¼-in. stainless steel valves, tubing, and other required fittings. Attached to the inside surface of each end flange was a 1½ in. sintered stainless-steel disk, 0.125 in. thick, with a maximum pore size of 100 microns. The physical parameters and operating conditions of the linear flow model are listed in Table 3.1.

TABLE 3.1
PARAMETERS OF RESERVOIR MODEL

Pressure (operating)	1112 psia
Temperature	123°F (51°C)
Length of Porous Medium	23.46 in. (59.6 cm)
Porosity	40.3%
Cross-sectional area	1.975 in. ² (12.73 cm ²)
Pore Volume	19.4 in. ³ (318 cc)
Permeability to brine	600 md



* Filter

Schematic Diagram of Apparatus Used for CO₂ Mobility Study

FIG 3.1

The model was mounted horizontally in an insulated box where the temperature was maintained at characteristic reservoir temperatures by light bulbs controlled by a thermostat (Johnson Controls, model A19AAF-12). Internal air circulation was maintained by a small blower (Dayton, model 1C939).

Pressure at the inlet of the model was measured by a 0-2000 psi gauge (Heise, model CM-29064) accurate to ± 2 psig. Pressure drop across the model was measured by a transducer (Validyne, model CD-223) that was protected from overpressure by a rupture disc in a parallel line.

3.1.2 Carbon Dioxide

A 48.8 in.³ (800 cc) stainless steel (304) rodded-piston transfer cylinder (Welker Engineering, sample cylinder style CP-2) served as the reservoir for carbon dioxide. Initially filled with liquid CO₂ from an inverted commercial cylinder, the reservoir was placed beside the model in the temperature-controlled box and brought to the same temperature.

To force carbon dioxide from the transfer cylinder, high-pressure nitrogen was admitted to one side of the piston (see Figure 3.1). As CO₂ flowed from the other end of the cylinder, the position of the moving piston was indicated by the length of the attached calibration rod that protruded from the end of the cylinder.

3.1.3 Effluent Collection

As water and carbon dioxide flowed from the model, they were separated in the accumulator. That vessel was wrapped with heating tape which kept it at 127°F to prevent condensation of liquid carbon dioxide.

Gas was passed through valve V-7 to a "Wet-Test" meter (GCA Precision Scientific). The valve (Whitey, SS-14DKM4-S4) had been modified

to serve as a back-pressure regulator. (The modification is described below).

Liquid was withdrawn from the bottom of the accumulator through valve V-10 which, like V-7, was also a pressure regulator.

Besides permitting gas and liquid to be separated, the accumulator served to dampen fluctuations in the downstream pressure. Small volumes of fluid could be withdrawn without appreciably changing the pressure-drop across the model. If gas was inadvertently withdrawn too rapidly, the system pressure would drop only slightly.

3.1.4 Modification of Valves

The valves, V-7 and V-10, had unthreaded sliding stems that facilitated their adaptation to act as pressure regulators. Also, the stems were smaller in diameter than the seats, a condition necessary for proper control. To modify the valves, the internal stem linkages were removed and replaced with coil springs which held the valves closed. After modification, each valve was installed in the system so that the upstream pressure was beneath the seat. When the pressure rose, it provided a force to oppose the spring force, and the valve opened to allow flow and a subsequent decrease in pressure. The handles of the valves were connected by threads to the bonnets and could be adjusted. Because the springs pressed against the inside of the handles, this adjustment changed the pressure at which the valve would open.

3.2 Procedure

3.2.1 Preparation of Model

One flange was bolted in place and the model was supported vertically with the open end up. A 1-cm layer of glass beads (Potter

Industries, type P, -70 +150 Tyler mesh) was carefully poured in using a funnel equipped with a long stem. On top of this was poured a 0.5-cm layer of -150 +200 mesh beads, then the model was filled with the silica flour. The silica flour (Midland Sand Co.) was nominally 20-micron and had been elutriated with water to remove most particles smaller than 10 microns.

To the upper flange was bolted a 12-in. length of pipe, and additional silica flour was poured into it while the model was struck firmly and repeatedly with a wooden mallet.

Air trapped in the model was purged with CO_2 at low pressure; then the CO_2 was removed by flowing pH 10.6 brine (3% NaCl by wt., 100 ppm Ca^{++}) through it while the outlet was connected to an aspirator. When the model was saturated with water, the upper section of pipe was removed, layers of glass beads were placed on top of the wet silica flour, another perforated stainless plate was placed on top of the beads, and the second flange was bolted in place.

The model was then mounted horizontally and flooded with deionized water to completely remove the brine; then it was flooded with a crude oil at 124°F to irreducible water saturation. The brine that had been produced during the waterflood was analyzed for chloride ion, Cl^- , by titration with silver nitrate solution to determine porosity and pore volume.

The model was finally flooded with brine until no more oil was produced. The residual oil saturation was 0.36.

3.2.2 Start-up

To minimize gravity segregation within the sand pack, the model was revolved 180° about its longitudinal axis every 30 minutes for several

hours before the experiment was begun. The temperature of the box containing the model and the CO₂ reservoir was set and allowed to become constant. The following steps were then taken to establish the desired system pressure:

1. Carbon dioxide was bled through valve V-9 until the pressure of the system was 1100 psig. The bypass valve, V-4, remained open to prevent damage to the transducer.
2. With valve V-8 still closed, the pressure inside the accumulator was increased to 1100 psig with nitrogen, then valve V-6 was closed and valve V-8 was opened to equalize the pressures in the accumulator and the rest of the system.
3. Valve V-5 was opened next and the nitrogen pressure was increased until the piston in the CO₂ reservoir advanced enough to raise the system pressure to 1115 psig. Valve V-5 was left open, so the CO₂ pressure would remain constant during the experiment.
4. The bypass valve, V-4, was finally closed and valve V-2 was opened to raise the pressure in the model to 1115 psig. Gas was bled from the accumulator through valve V-7 until the transducer showed that a differential pressure of 10 psid existed across the model.
5. The final step was to open valve V-1 to start the flow of CO₂ through the model.

3.2.3 Operation

Within seconds of opening valve V-1, the inlet pressure (indicated by PI-1) had dropped to 1110 psig, but then it remained constant throughout the flood. The pressure-drop across the model was maintained at 10

psid by manually adjusting valve V-7 and bleeding gas through the Wet-Test meter. Continual adjustment was required, because as the water saturation decreased, the flow of gas through the model increased.

3.2.4 Data Collection

The length of the position-indicator rod on the cylinder holding the CO₂ was measured frequently to determine the rate of fluid injection. The volume of gas leaving the model was measured by reading the Wet-Test meter.

The volume of water produced during each time interval was determined by draining the liquid from the accumulator (valve V-10) into a tared bottle and then weighed. Any gas which escaped with the water was vented to the Wet-Test meter and thus measured.

3.2.5 Data Analysis

The relative permeabilities of water and CO₂ as functions of water saturation were calculated using a procedure based on the original work of Johnson, et al. [87] with modifications proposed by others [86, 89,93]. The data required for the calculations are cumulative volumes of injected CO₂ and produced water, the rate of CO₂ injection, viscosities of water and CO₂, and the physical properties of the porous medium such as its length, cross-sectional area, porosity and initial saturation with respect to water.

Interpretation of the data was complicated by their erratic nature which was due to fluctuations in pressure-drop across the model during the experiment. (The resulting "data-scatter" is evident in Figure 3.2). Controlling the pressure drop at 10 psid was difficult,

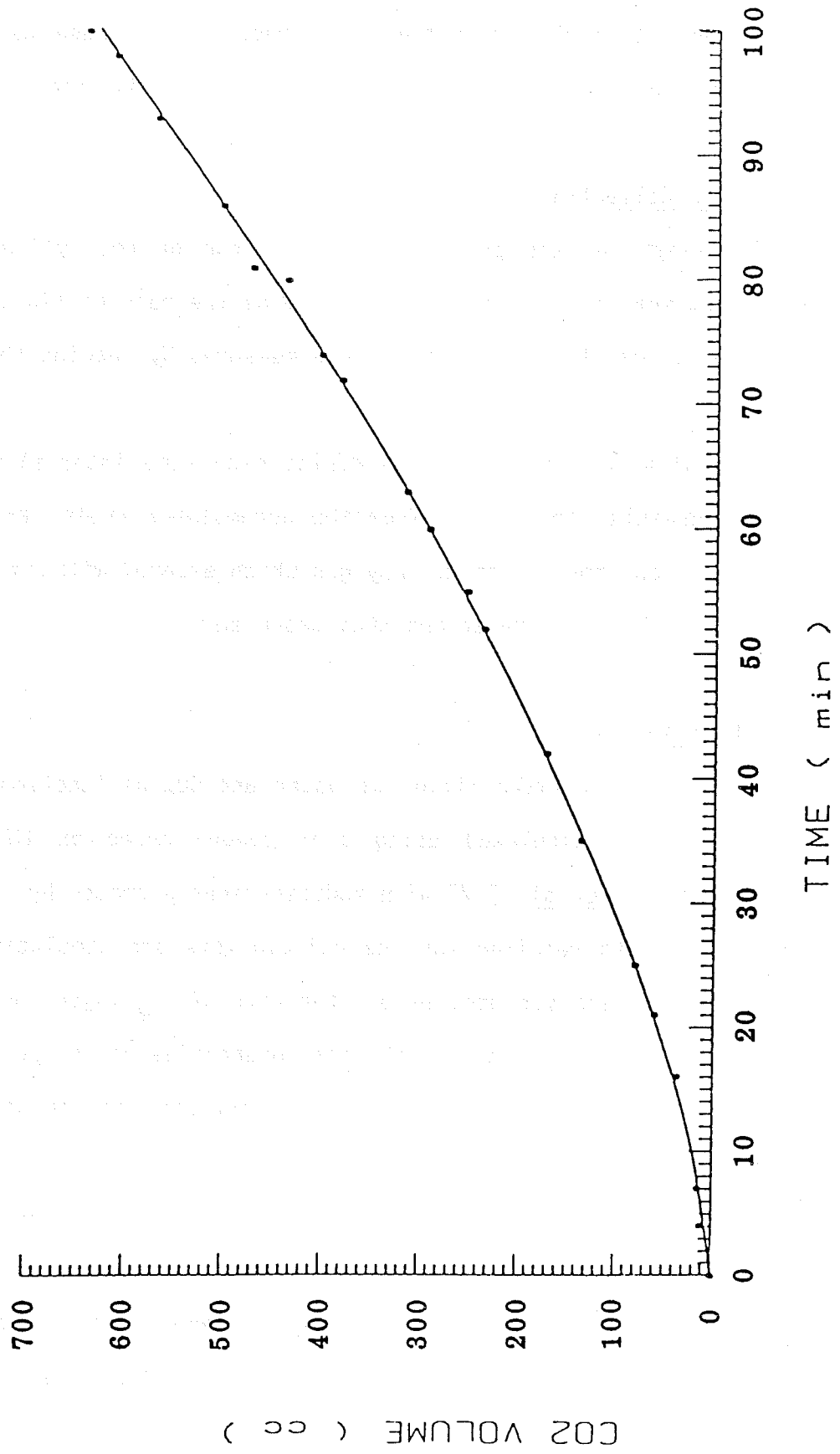


FIG 3.2: CUMULATIVE VOLUME CO₂ INJECTED

because the CO₂ flow rate was continually increasing during the experiment and because the system pressure was so high (1112 psia). Thus, small changes in the flowrate caused small changes in the downstream pressure, but large percentage changes in the pressure difference.

To minimize the problems arising from the erratic nature of the data, the data were smoothed by curve-fitting with appropriate equations. The cumulative volume of injected CO₂ was fit with an equation of the form:

$$G = d + at + (b)\exp(ct) \quad (3.1)$$

where G is cumulative volume of CO₂ at reservoir conditions and t is time (min). The agreement between the equation for injected gas and the experimental data may be seen in Figure 3.2.

The cumulative volume of produced brine was fitted with two equations of the form of Eq. 3.1. This was done to ensure that the inflection point (corresponding to gas breakthrough) was accurately represented (see Figure 3.3).

The equations for cumulative water production were differentiated with respect to time to get rate expressions of the form:

$$dL/dt = a_1 - (b_1c_1)\exp(b_1t) \quad (3.2)$$

Similarly, the equation for cumulative CO₂ volume was differentiated with respect to time to get an expression for CO₂ injection rate, q(t), having the form of Eq. 3.3,

$$dG/dt = q = a + (bc)\exp(ct) \quad (3.3)$$

(The equation for injection rate, q(t), is compared with measured rates in Figure 3.4. The agreement is good, as it should be). Dividing Eq. 3.2 by Eq. 3.3 gives the derivative of L with respect to G, i.e.,

$$\frac{dL}{dG} = \frac{dL/dt}{dG/dt} = \frac{a_1 - (b_1c_1)\exp(c_1t)}{a + (bc)\exp(ct)} \quad (3.4)$$

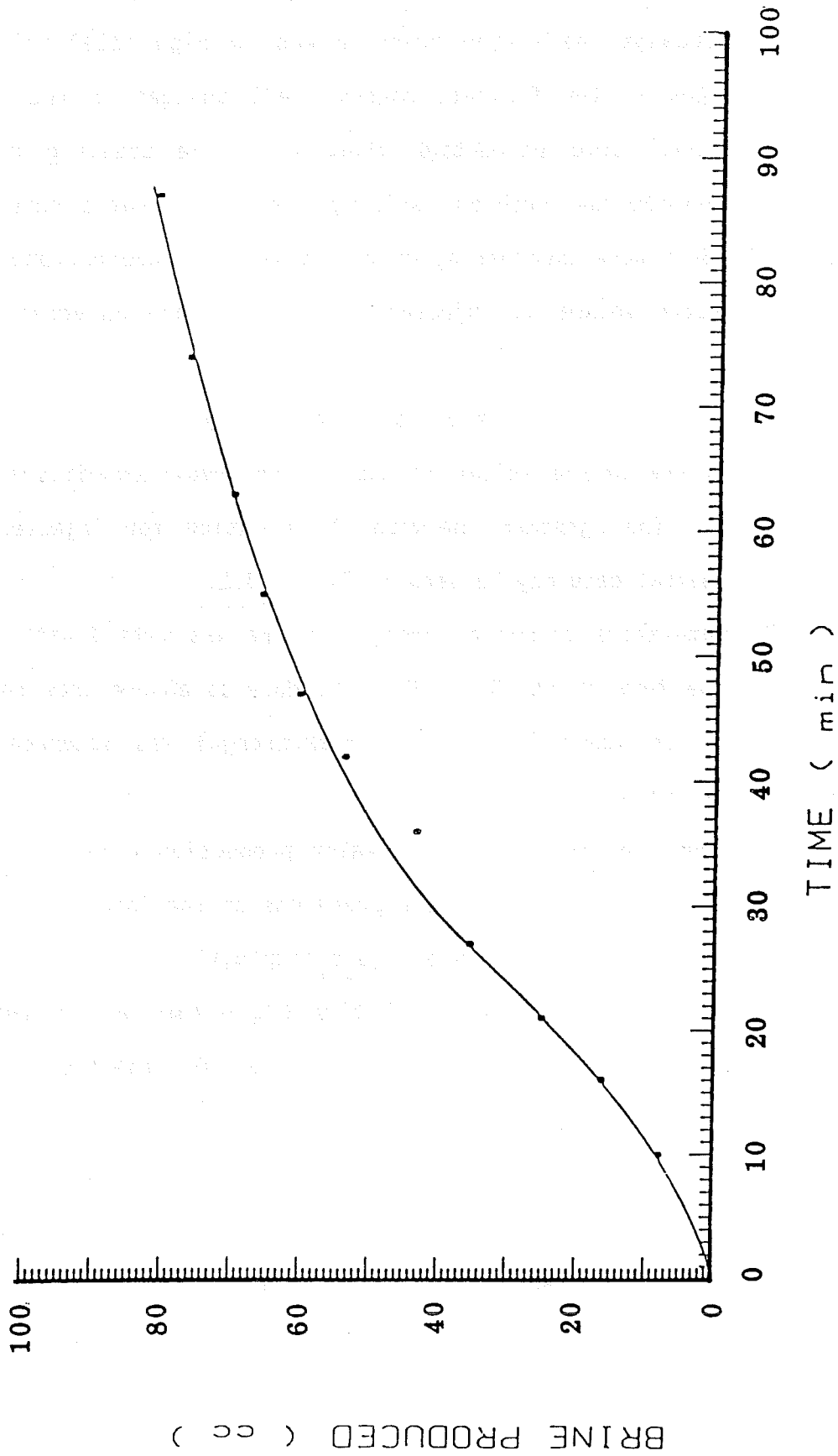


FIG 3.3: CUMULATIVE BRINE PRODUCED

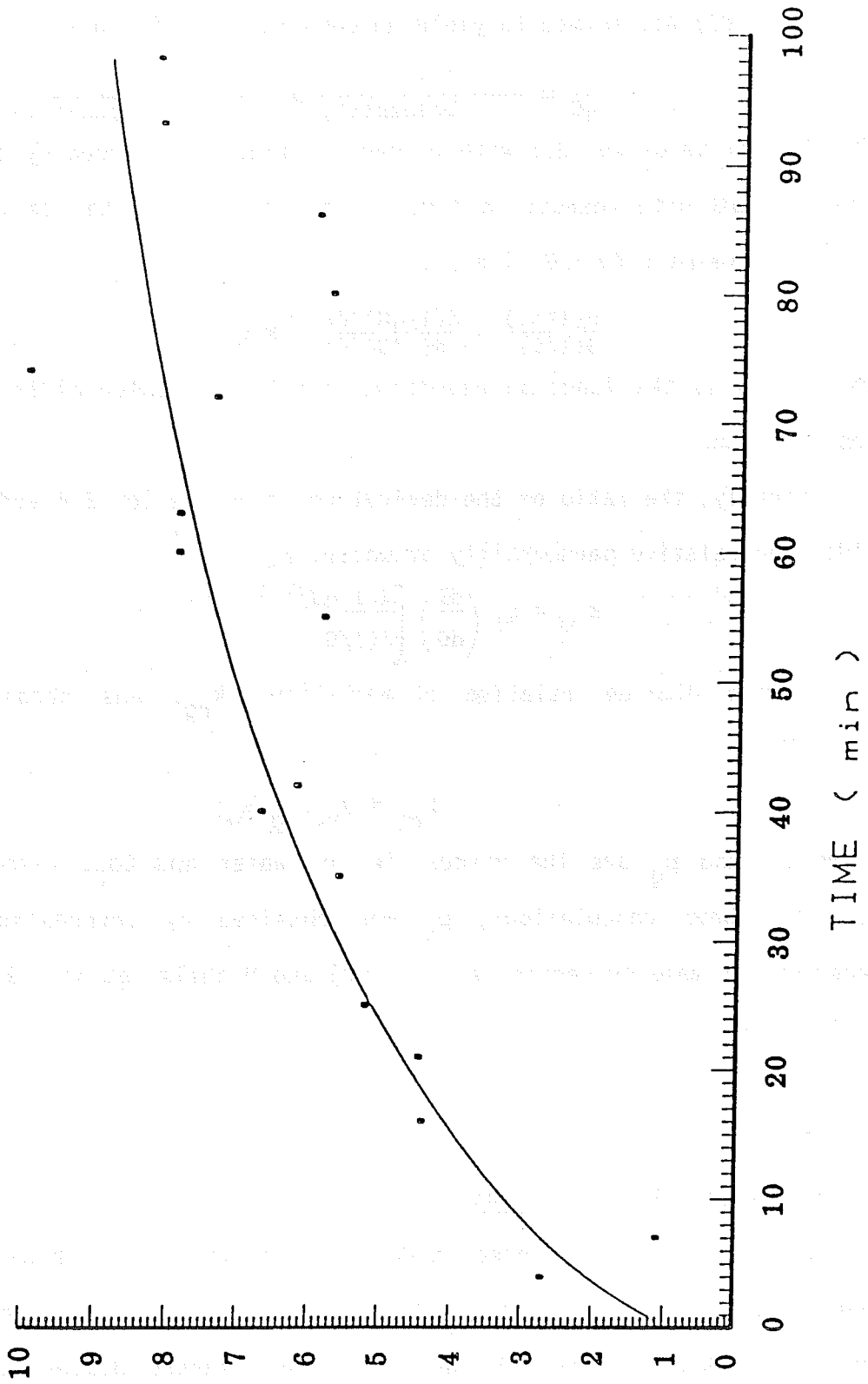


FIG 3.4: RATE OF CO₂ INJECTION

CO₂ INJECTED (CC / MIN)

Next, the product of the reciprocals of $q(t)$ and cumulative CO_2 injection (G) was formed to yield an equation of this form:

$$\frac{1}{qG} = \frac{1}{a - (bc)\exp(ct)} \times \frac{1}{d + at + (b)\exp(ct)} \quad (3.5)$$

The derivative of Eq. 3.5 with respect to time was divided by the derivative of $1/G$ with respect to time giving, in effect, the derivative of $1/qG$ with respect to $1/G$, i.e.,

$$\frac{d(1/qG)}{d(1/G)} = \frac{d(1/qG)/dt}{d(1/G)/dt} = F(t) \quad (3.6)$$

where $F(t)$ is the function resulting from the indicated differentiation and division.

Finally, the ratio of the derivatives given by Eq. 3.4 and 3.6 provided the relative permeability of water, k_{rw} :

$$k_{rw} = q_i \left(\frac{dL}{dG} \right) \left[\frac{d(1/qG)}{d(1/G)} \right]^{-1} \quad (3.7)$$

The carbon dioxide relative permeability, k_{rg} , was obtained from Eq. 3.8:

$$k_{rg} = k_{rw} (\mu_g / \mu_w) \quad (3.8)$$

where μ_w and μ_g are the viscosities of water and CO_2 , respectively. For the above calculations, μ_g was obtained by interpolation from measurements made by Kestin, et al. [90] and Michels, et al. [91] on CO_2 at 122°F over a range of pressures.

3.3 Results

3.3.1 Relative Permeabilities

Using the data for injected CO_2 and produced liquid obtained after breakthrough of CO_2 occurred, the relative permeability curves were determined (see Figures 3.5 and 3.6). For reasons discussed below, the volume of injected gas was corrected for the amount which dissolved

in the water and oil; thus the values for cumulative gas that were used in calculating the permeabilities are not those depicted in Figure 3.2.

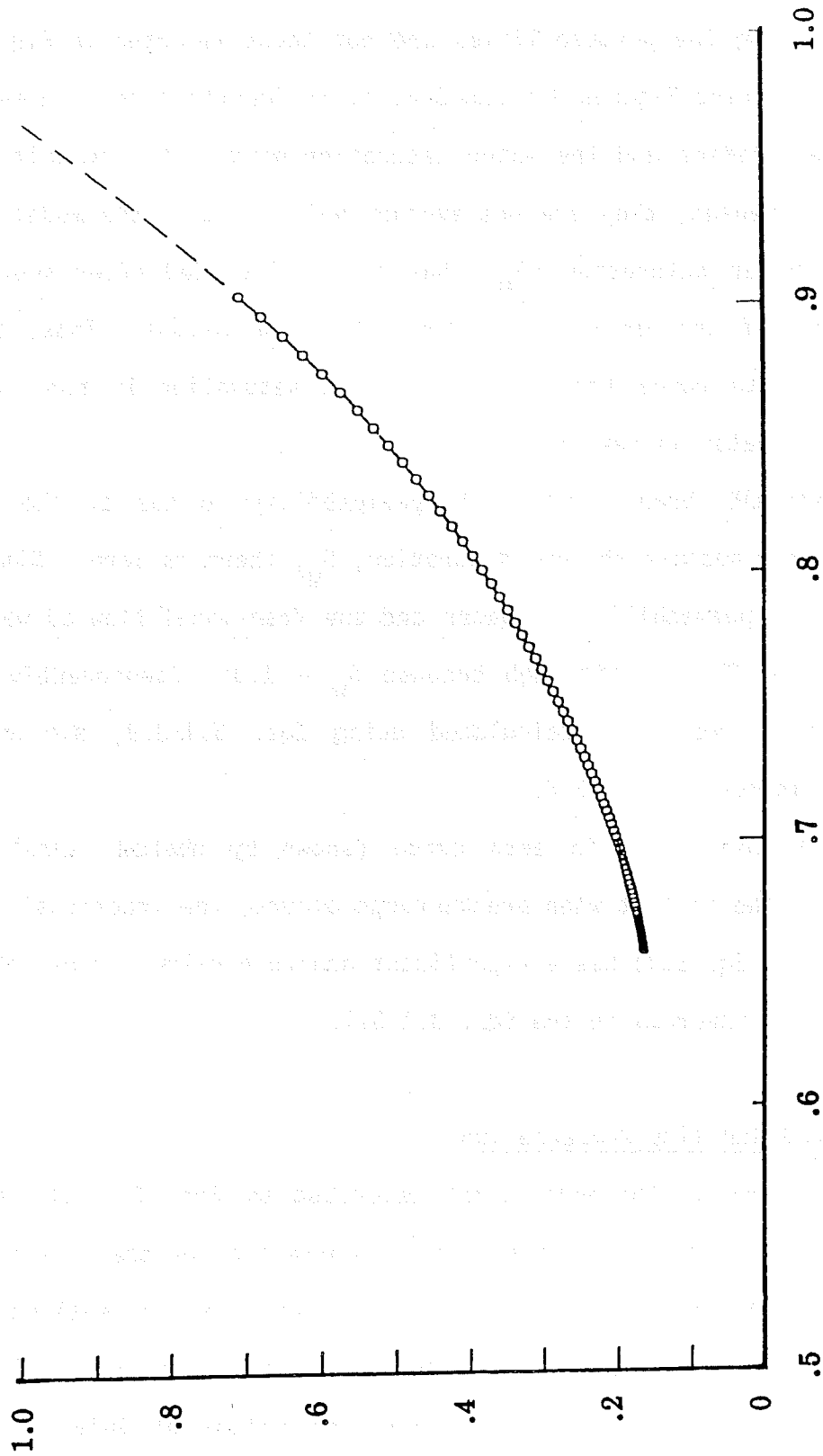
In examining Figures 3.5 and 3.6, it is important to note that both the permeabilities and the water saturation pertain to the exit face of the porous medium; they are not average values within the model. Moreover the water saturation (S_{wL}) has been calculated after subtracting the volume of the immobile oil from the pore volume. Thus, S_{wL} has been scaled to range from 1.0 if the gas saturation is zero (at $t=0$) to 0 if all water is removed.

Before CO_2 breakthrough, the permeability to gas at the model's exit is zero, because the gas saturation, S_g , there is zero. Similarly, the relative permeability to water and the fractional flow of water are 1.0 prior to CO_2 breakthrough because $S_w = 1.0$. Consequently, these permeabilities were not calculated using Eqs. 3.1-3.8, nor are they shown on Figures 3.5 and 3.6.

The discontinuity in each curve (shown by dashed lines) arises because, at the instant when breakthrough occurs, the fractional flow of gas (dG/DL in Eq. 3.7) has a significant non-zero value. Thus, the discontinuity is inherent in the Eqs. 3.1-3.8.

3.3.2 CO_2 Solubility Compensation

Proper use of the math model described by Eqs. 3.1-3.8 requires that the expression for injected gas be corrected for the portion which dissolves in the water and oil. The reason is that the math model was developed for waterfloods or immiscible gas drives, and the total volume of produced fluid is assumed to equal the volume of injected fluid. This causes a problem when CO_2 is the injected fluid, because the injected volume (as depicted in Figure 3.2) is significantly larger



WATER SATURATION AT OUTLET

FIG 3.5: RELATIVE PERMEABILITY OF WATER IN PRESENCE OF OIL

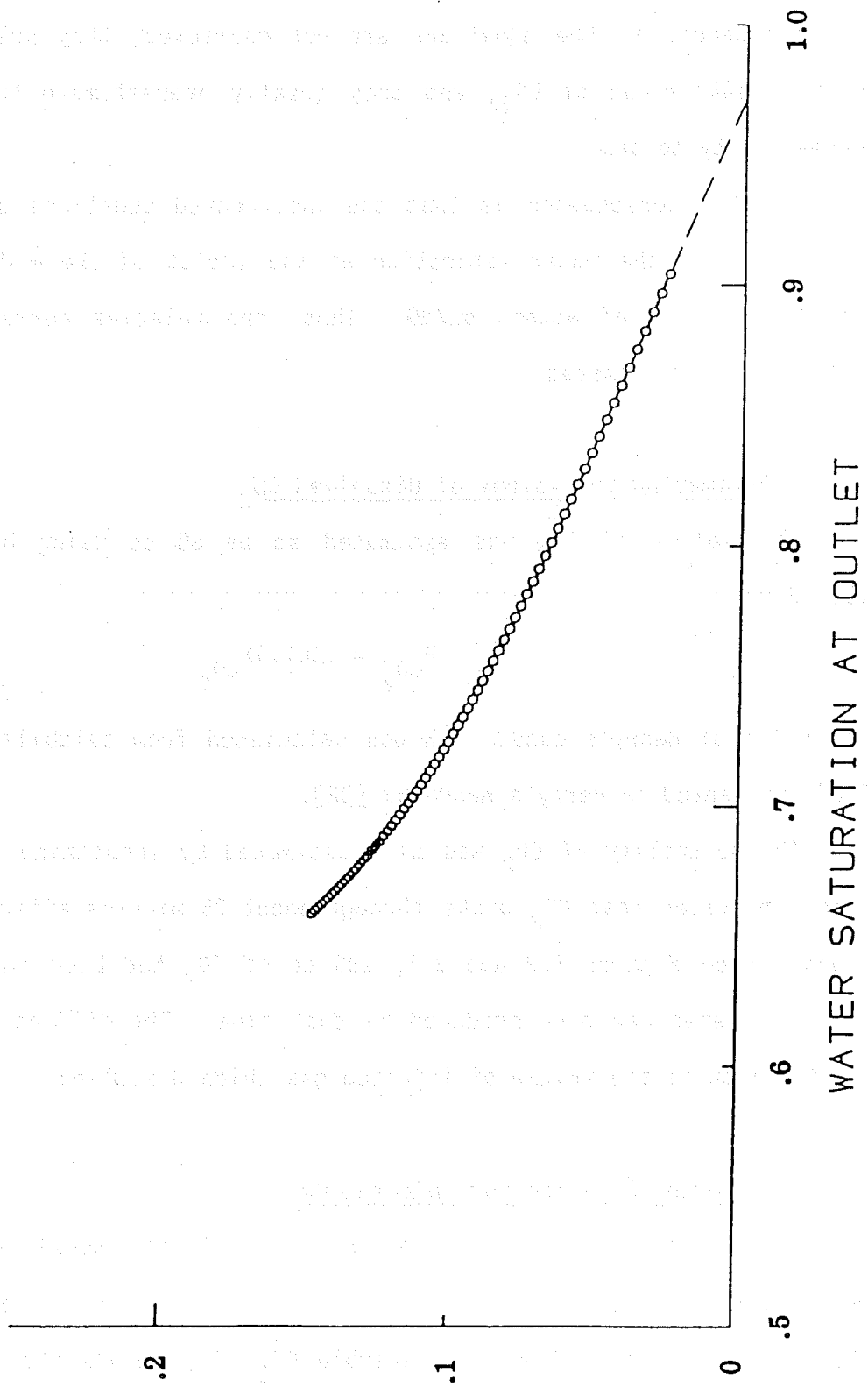


FIG 3.6: RELATIVE PERMEABILITY OF CO₂ IN PRESENCE OF OIL

than the produced volume, owing to carbon dioxide's solubility. As a consequence, if the equations are not corrected, they predict immediate breakthrough of CO₂, and they greatly overestimate the relative permeability to gas.

Another consequence is that the uncorrected equations also underestimate both the water saturation at the outlet of the model and the fractional flow of water, dL/dG. Thus, the relative permeability to water is underestimated.

3.3.3 Estimating the Volume of Dissolved CO₂

The volume of CO₂ was estimated to be 85 cc using Henry's law (Eq. 3.9).

$$P_{CO_2} = .00714X_{CO_2} \quad (3.9)$$

The value of Henry's constant H was calculated from solubility data at 122°F presented in Perry's Handbook [92].

The solubility of CO₂ was also estimated by inspecting Figure 3.7 which indicates that CO₂ broke through about 35 minutes after the flood began. From Figures 3.2 and 3.3, 130 cc of CO₂ had been injected and 45 cc of water had been produced by that time. The difference, 85 cc, was taken to be the volume of injected gas which dissolved.

3.3.4 Corrected Equation for Injected CO₂

Because the rate at which CO₂ dissolves in the model is unknown, two assumptions were made: (1) After CO₂ breakthrough, no more CO₂ dissolves; thus the volume of insoluble CO₂ (G_i) equals the cumulative injected volume (G) less the dissolved volume (85 cc):

$$G_i(t) = G(t) - 85 \quad t \geq 35 \text{ min} \quad (3.10)$$

where G(t) is given by Equation 3.1. (2) Before breakthrough, the

volume of insoluble CO_2 that was injected equals the volume of water produced (L_p):

$$G_i(t) = L_p(t) \quad t \leq 35 \text{ min} \quad (3.11)$$

These equations are depicted in Figure 3.8.

3.3.5 Curve Fitting Equations

If the measured values for injected gas are "smoothed" by fitting them with an equation which has discontinuities, or an equation which has discontinuities in either its first or second derivatives, the relative permeabilities will not be continuous functions of water saturation. This can be seen by inspecting Eqs. 3.7 and 3.8.

Another constraint is that the equation for injected gas (G_i) cannot have a first derivative which is negative. By definition (Eq. 3.3), if the first derivative of G_i is negative, the injection RATE, q , is negative. This implies that gas is being withdrawn instead of injected. Moreover, the relative permeability to gas is predicted to be negative because dL/dG (Eq. 3.4) is negative and this is a factor in Eq. 3.7.

A third requirement is that the second derivative of G_i should be greater than zero. That is because the flowrate, $q(t)$, increases continuously as the water saturation decreases and $q(t) = dG_i/dt$, by definition (Eq. 3.3). Consequently, dq/dt must be positive throughout the time domain so the second derivative of G_i must be positive since

$$\frac{dq}{dt} = \frac{d^2G_i}{dt^2} \quad (3.12)$$

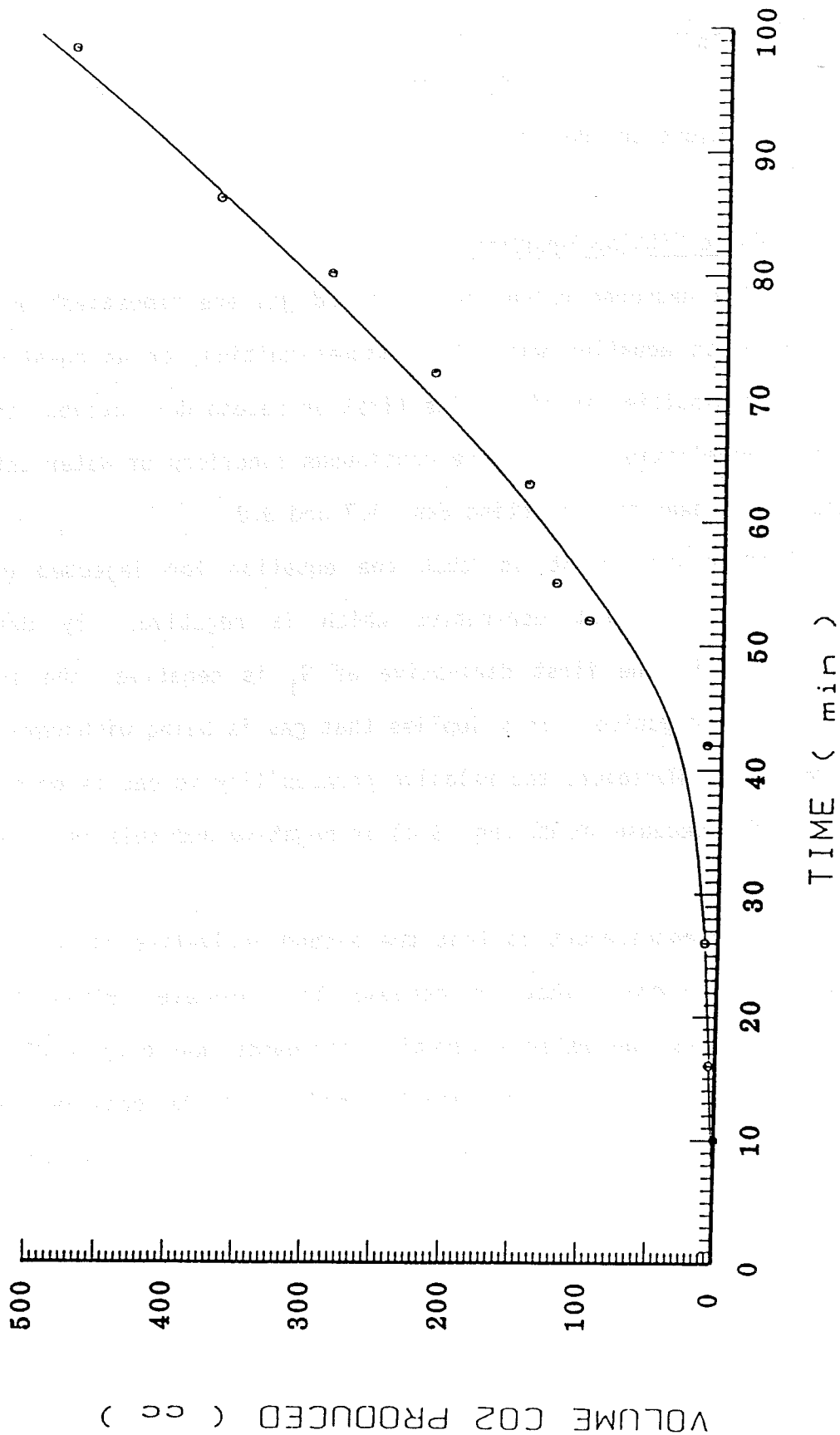


FIG 3.7: CUMULATIVE VOLUME CO₂ PRODUCED

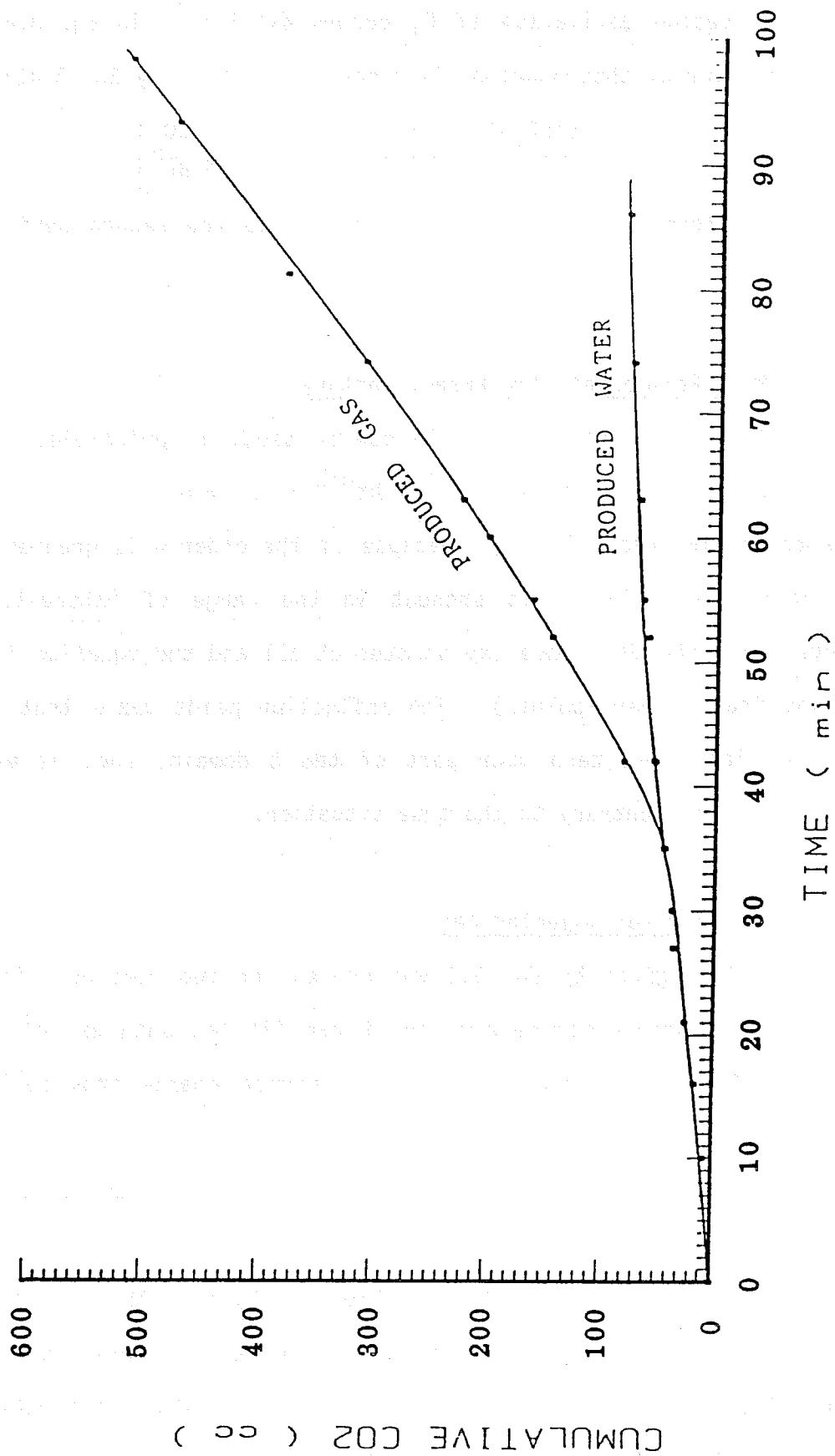


FIG 3.8: CUMULATIVE VOLUME INSOLUBLE CO₂

The second derivative of G_i occurs explicitly in Eq. 3.6 because the numerator of that equation is computed as shown by Eq. 3.13:

$$\frac{d(1/G_i q)}{dt} = \frac{-1}{(G_i q)^2} \left[G_i \frac{dq}{dt} + q \frac{dG_i}{dt} \right] \quad (3.13)$$

The first term in square brackets, dq/dt , is the second derivative of G_i (see Eq. 3.12)

3.3.6 Most Polynomials Are Unsatisfactory

Polynomials such as Eq. 3.14 can be used, in principle. But they

$$G_i(t) = at^n + bt^{n-1} + \dots + m \quad (3.14)$$

are generally unsatisfactory, because if the order n is greater than 2, an inflection point(s) is present in the range of interest. (This occurs when the data have any scatter at all and the equation is forced to fit four or more points). The inflection point means that d^2G_i/dt^2 will be less than zero over part of the t domain, and, as explained above, this is contrary to the true situation.

3.3.7 Equation for Injected Gas

The form given by Eq. 3.1 was chosen for two reasons. First, it has four adjustable parameters, so it can fit the data exactly at four points. Second, its second derivative cannot change from positive to negative.

Obviously, the equation for G_i should include the point (0,0), since the injected volume is zero at time zero. However, to obtain a better fit to the data for times following CO_2 breakthrough, this constraint was not applied. This is permissible only because the relative permeability to gas, at the model's exit, is zero until breakthrough. Similarly, the relative permeability to water is 1.0 until breakthrough.

3.3.8 Equation for Produced Water

Figure 3.3 shows that the flowrate of water increases until gas breakthrough (point B), then it decreases. This is reasonable when one considers that the relative permeability to gas increases with time, so the injection rate in this constant pressure-drop experiment increases, too. In accord with equation 3.11, the rate of water production must increase. By contrast, the water flowrate decreases after gas breakthrough occurs, because both the water saturation and the relative permeability to water decrease.

Because of the inflection point in the curve for produced water (see Figure 3.3), a single equation like Eq. 3.1 cannot satisfactorily fit the data over the entire time domain. Consequently, one equation like Eq. 3.1 was used for the period after gas breakthrough and another for the period before it.

Ideally, the curves for injected gas and produced water should have the same value at the breakthrough point B and their first derivatives should be equal. This would ensure that the curves would join smoothly as depicted in Figure 3.8. However, this is difficult to accomplish using equations like Eq. 3.1 because they have only four parameters. The constraints on the curves at point B leave only two degrees of freedom. Consequently, the equations can be made to fit the data exactly at only two other points.

3.3.9 Alternative Forms

Two forms that will be tested in the future to fit the data for produced liquid are given by Eqs. 3.15 and 3.16.

$$L_p = (a)\exp[-(c)\exp(-bt)] \quad (3.15)$$

$$L_p = 1 - \ln[1 + (c)\exp(-bt)] \quad (3.16)$$

Each has the advantage that one inflection point, and only one, is inherent in their form.

SECTION FOUR
MISCIBLE DISPLACEMENT

4.1 Apparatus

4.1.1 Reservoir Condition Flow Model

Miscible oil displacement experiments were conducted in apparatus consisting of a tubular flow model, filter system, constant temperature box, three pressure gauges, a differential pressure transducer and a transfer cylinder. A schematic diagram of the apparatus is shown in Figure 4.1. The flow model is 54.3 in. (138 cm) long made from 1½ in. NPS, schedule 40, seamless, type 316L stainless-steel pipe. The ends are closed with 900-pound flanges welded to the pipe. The inside diameter of the column is 1.6 in. (4.03 cm) and, the cross-sectional area of the model is 2.0 in.² (12.8 cm²). The flange gaskets are teflon-stainless spiral type gaskets. The detail of the inlet section of the model is shown in Figure 4.2. A sintered stainless-steel disk confines the fine, unconsolidated sand packing. The column is filled with silica sand, elutriated to obtain a size range of 20 μm to 80 μm. Pore volume of the model was determined to be 42.0 in.³ (688 cm³) by fluid displacement tests, and the porosity was calculated to be 39.2 percent. The model is mounted in a constant temperature chamber, in which air is circulated to maintain the temperature of the model.

The fluid entering the column is filtered through two different types of filters in series. The first was a sand filter and second, a millipore-filter.

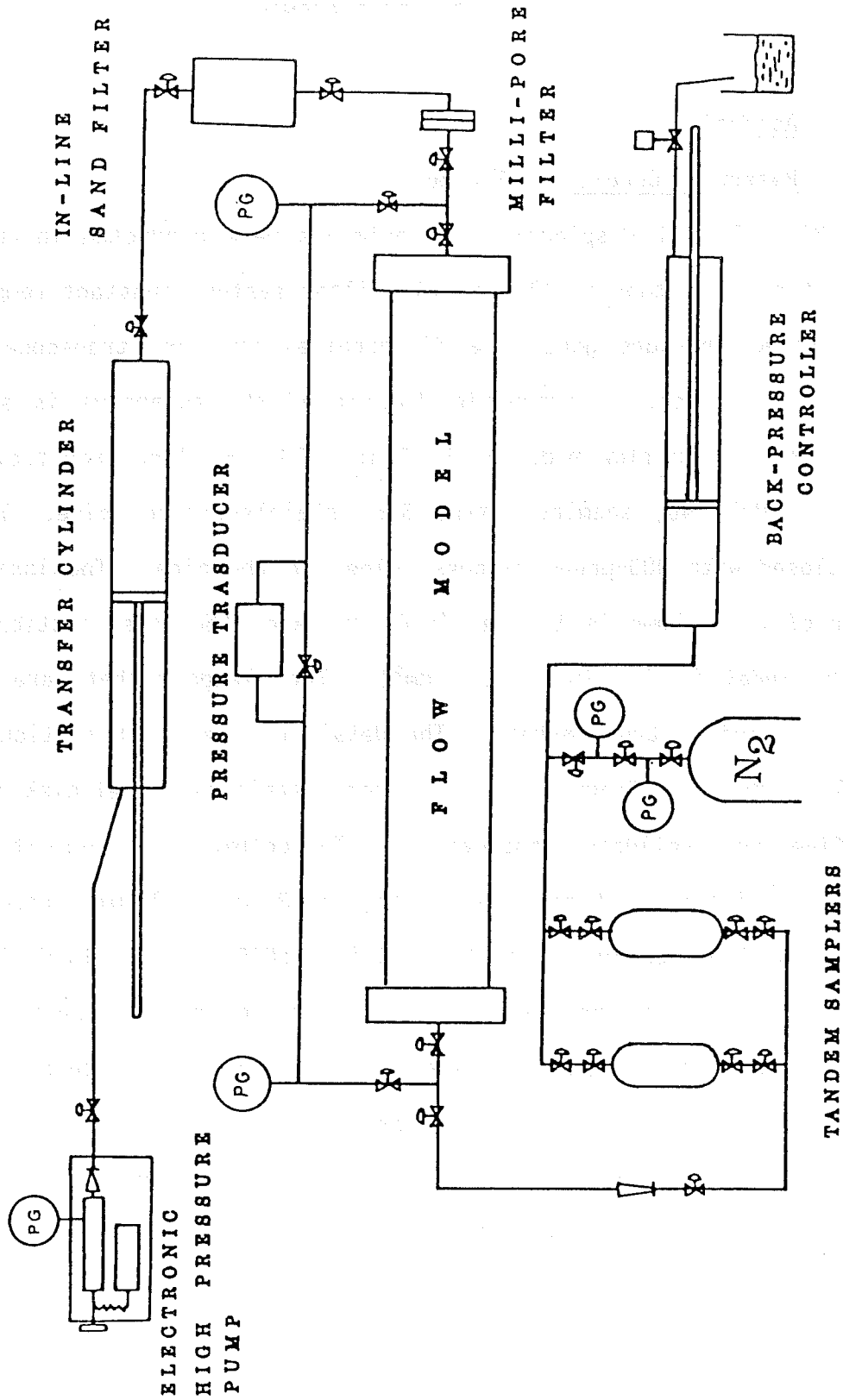


FIG 4.1: Miscible Displacement Apparatus

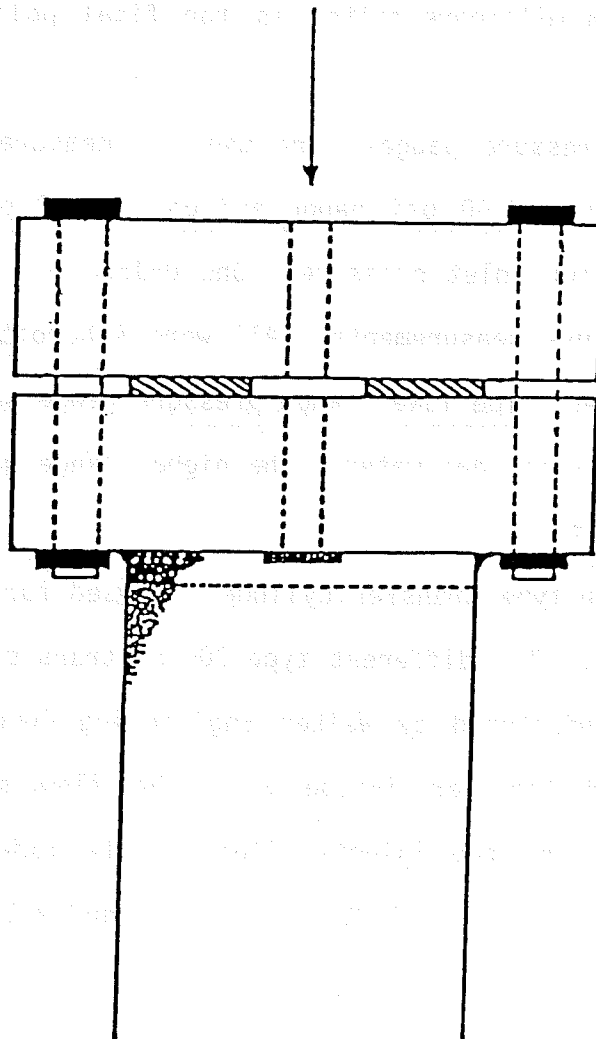


FIG 4.2: MODEL ENTRANCE CONSTRUCTION

The upstream sand filter is designed to remove any particles or precipitates which possibly exist in the injection fluid. A diagram of the sand filter is shown in Figure 4.3. This filter is filled with + 20 μm silica-flour supported by a sintered-metal disk. To prevent channeling or shifting of the particles, glass wool is placed on top of the silica flour packing.

A 10 μm millipore-filter is for final polishing of the injected fluids.

Three pressure gauges were used to measure the inlet and outlet pressures. One 0-60 psi gauge and one 0-1500 psi gauge were alternatively used for inlet pressure. One 0-1500 psi gauge was used for all outlet pressure measurements. All were Ashcroft, Maxisafe gauges with type 316 tubes. The lower range pressure gauge was used when saturating the model with oil and water. The higher range gauges were used for CO_2 injection tests.

A piston-type transfer cylinder is used for the injection of fluid in the model. Two different type 304 SS transfer cylinders, 500 cc and 2000 cc manufactured by Welker Engineering Company, were used. They were located together inside with the flow model, the temperature cabinet to bring the injected fluid to the model temperature prior to injection. Fluid was injected by pumping hydraulic oil into one side of the piston in the transfer cylinder.

4.1.2 Injection Pump

For the injection of hydraulic fluid into the transfer cylinder, a modified Ruska pump was used. The body of the pump was manufactured by the Ruska Instrument Company in Houston, Texas. It was equipped with a

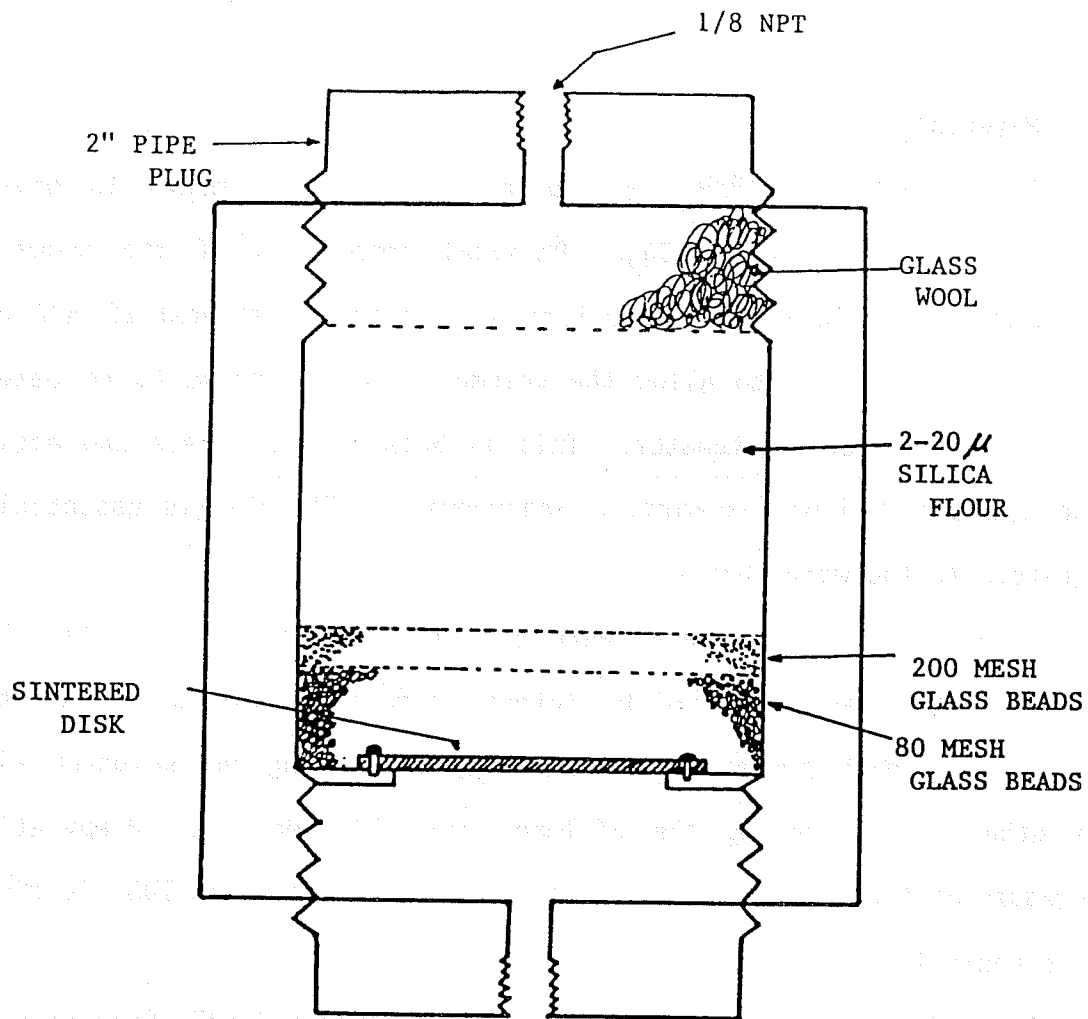


FIG 4.3: Injected Fluid Filter

totally electronically controlled drive train developed at New Mexico State University. It can be controlled to run in either a constant rate, constant pressure or constant differential-pressure mode.

4.2 Materials

Pure n-octane, 71°API, was used for all experiments to ensure miscibility with injected CO₂. Physical properties of the n-octane are given in Table 4.1. The octane was colored with Red LS 672 dye (Tricon Colors Inc.) to allow the volume of oil produced to be determined with a spectrophotometer. This is both more accurate and easier than the conventional volumetric measurement. The dye is essentially insoluble to the water phase.

Brine and deionized water were alternated in the experiments. The deionized water was prepared by reverse osmosis. Pore volume of the column after each process was checked by displacing one solution with the other and titrating the effluent for chloride ion. Preparation procedure of the brine solution which contained about 3.2% TDS, is given in Appendix A.

Three different types of surfactants, Pluradyne SF-27, Stepanflo-50 and Exxon LD 776-52 were evaluated. All are commercially available at present. Specific information on surfactant properties is given in Table 4.2. Surfactant solutions were mixed using a magnetic stirrer for several hours.

TABLE 4.1

PHYSICAL PROPERTIES OF N-OCTANE

Properties	n-Octane
B.P. (°F)	257.6
Density (g/ml)	0.7025
M.W.	114.23
Formula	$\text{CH}_3(\text{CH}_2)_6\text{CH}_3$
API Gravity @100°F	71°
Critical Temperature (°F)	565
Critical Pressure psia	364

TABLE 4.2

MOBILITY CONTROL SURFACTANTS

	<u>Pluradyne SF-27</u>	<u>Stepanflo-50</u>	<u>Exxon LD 776-52</u>
Company Name	BASF Wyandotte	Stepan Chem Co.	Exxon Co.
Chemical Formula	Ethoxylated Alcohol	Sulfate Ester of Alcohol	Sulfonate
Concentration, %	0.5	0.5	0.5
Solution	Std. Brine	Std. Brine	Std. Brine

4.3 Procedure

4.3.1 Saturation of the Model

In preparation for an experiment, the model is saturated with n-octane and brine containing 100 ppm calcium ion and 30,000 ppm sodium chloride to produce an environment similar to that encountered in a virgin oil reservoir. Brine is injected first and then displaced to its residual saturation with n-octane. The oil and water saturations were calculated by material balance. At the end of the experiment, the model was flooded with one or more pore volumes of deionized water, and the residual saturations were rechecked by titration of the effluent water.

4.3.2 Water and Surfactant Flood

After saturating the model with brine, a waterflood was initiated. This simulates the primary and secondary oil recovery processes. A differential pressure of 5 psi/ft was maintained through the waterflood. Initially, the waterflood produced water-free oil as is customary. After water breakthrough, oil production decreased abruptly until only the water phase was produced. After the waterflood, the oil saturation was checked by the injection of deionized water to obtain a baseline for the conventional miscible process. CO₂ was then injected and additional oil recovery recorded. For the CO₂ mobility control experiments, the model was flooded with one pore volume of the prescribed surfactant solution at a differential pressure of 2.0 psi/ft. No oil was produced during the surfactant injection phase.

4.3.3 Carbon Dioxide Tertiary Flood

The model was maintained at reservoir conditions of 1300 psig and 100°F for the CO₂ floods. During CO₂ injection, the pressure differential gradually increased from 2 to 10 psi/ft. Carbon dioxide was supplied from a transfer cylinder that was located inside the constant temperature box. To fill the transfer cylinder, it was packed in ice and then charged from a CO₂ tank configured to supply a flow of liquid CO₂. The model was pressurized with CO₂ to 1300 psi before opening the outlet valve. Samples were then collected using the high pressure sample collecting system.

Three sample accumulators were alternated to achieve continuous operation. The maximum capacity of each sample accumulator is 40 cc. When an estimated 20 cc of fluid had been produced, a new accumulator was inserted. After installing to a new accumulator, it was pressurized with nitrogen to 1300 psi before opening the valve connecting it to the model. This procedure was done as quickly as possible, so as not to disturb the steady-state operation of the process. Each sample accumulator removed from the system was weighed and then connected to a wet test meter (GCA/Precision Scientific Co.). Pressure was reduced very slowly using a needle valve, and the produced CO₂ was recorded. During the pressure reduction process, the sample accumulator was kept inside the ice-bath to prevent the loss of liquids by evaporation.

4.3.4 Sample Analysis

The samples collected usually contained two layers, oil and water. To analyze the amount of oil in the sample, a spectrophotometer response to the red dye in the oil phase was used. The optimum wavelength,

determined for three different concentrations of oil diluted with octane was 515 nm. Using this wavelength, a calibration curve of the wt% oil versus absorbance was generated. Actual oil produced was determined by diluting the produced sample of red n-octane with pure n-octane. The measured absorbance of the diluted sample coupled with the known dilution ratio allowed the actual oil produced to be easily and accurately calculated.

For surfactant free samples, pure n-octane was used for dilution and no problems were encountered. In the case where surfactants were present, a third layer of emulsion formed between the oil and water phases. By substituting n-octanol followed by acetone as the diluent for n-octane, the two phases separated cleanly. The oil phase was then analyzed spectrophotometrically as before, using a different calibration curve.

4.4 Results

A total of four miscible displacement runs were conducted in the linear model. The results of these four runs are shown in Table 4.3 and Figures 4.4-4.7. Analyses of these data indicate no adverse effect on miscibility due to the presence of the surfactants, one run also reveals a dramatic improvement due to the decrease in CO₂ mobility. Together they offer strong support for the feasibility of utilizing mobility control additives in conjunction with carbon dioxide in field applications involving miscible displacement of oil with carbon dioxide. Each of the tests included a base waterflood prior to the initiation of the tertiary carbon dioxide recovery process. The comparable performance observed in

all four waterfloods attests to the reliability of the data and justifies a quantitative comparison of the experiments. Model characteristics as well as fluid saturations, indicative of the performance of the different mobility control additives, are summarized in Table 4.3. Referring first to Figure 4.4, the data represent a conventional CO₂ tertiary flood of a waterflooded light oil reservoir. It can be seen that the waterflood, represented by the data prior to CO₂ injection, recovered 0.5 PV of oil. This amount represented 76 percent of the oil initially in place and produced a residual oil saturation at the end of water flood of 0.16 PV. Both the recovery and the residual saturation are consistent with values expected in a waterflood of a light oil.

TABLE 4.3
MOBILITY CONTROL FLOODS

	Conventional CO ₂ Flood	I	II	Exxon LD 776-52	Pluradyne SF-27	Stepanflo- 50
S _{oi} ; cc		444	464	465	477	445
S _{oi} ; PV		.65	.67	.68	.69	.65
Waterflood						
Octane Produced:						
cc		350	352	364	342	350
PV		.51	.51	.53	.50	.51
S _{rowf} , PV		.15	.16	.15	.19	.16
CO ₂ Flood						
Octane Produced:						
cc		29	46	98	48	34
PV		.042	.067	.142	.070	.049

Injection of one pore volume of carbon dioxide ($T = 100^{\circ}\text{F}$; 1370 psi) followed by additional water produced only 7 percent PV additional oil. Laboratory miscible floods normally produce over 10 percent additional oil. The low oil recovery shown in Figure 4.4 is due largely to inefficient macroscopic oil displacement induced by an unfavorable mobility ratio that exists between carbon dioxide and oil. The larger than usual model diameter allowed the phenomenon to be observed. This phenomenon has not been reported for experiments conducted in long, slim tube models where CO_2 injection was not preceded by waterflood.

The results of the conventional CO_2 flood I are presented in Table I for comparison. This was the first experiment performed which could account for the lower oil recovery. Conversely conventional flood II was the last experiment and benefited from the improved ability of the operator. For comparison with the mobility controlled floods the average of floods I and II will be used.

The results presented in Figure 4.5 were obtained using Stepanflo-50 as a mobility control additive. Stepanflo-50 is a sulfated ethoxylated adduct of a linear alcohol. It is the most effective additive, having this chemical structure, identified in this program. As was the case in the conventional CO_2 flood, the preliminary waterflood produced 0.5 pore volumes of oil. Prior to injecting carbon dioxide the model was carefully flooded at low pressure drop 2 psi/ft, with a brine solution containing 0.5 percent Stepanflo 50. This surfactant does not reduce interfacial tension between n-octane and brine enough to encourage displacement of residual oil. This is indicated by the long period of surfactant injection without any oil production.

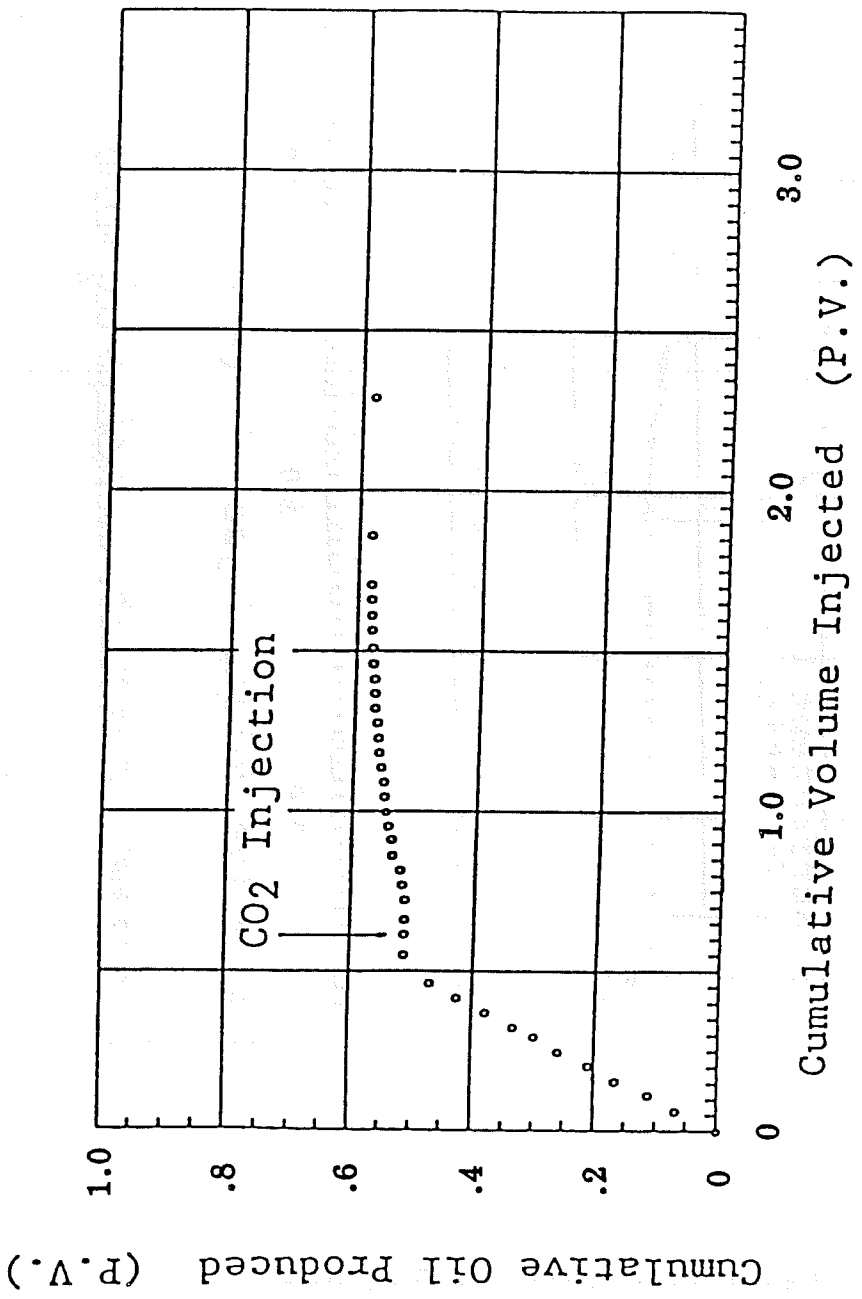


FIG 4.4: CONVENTIONAL CO₂ FLOOD

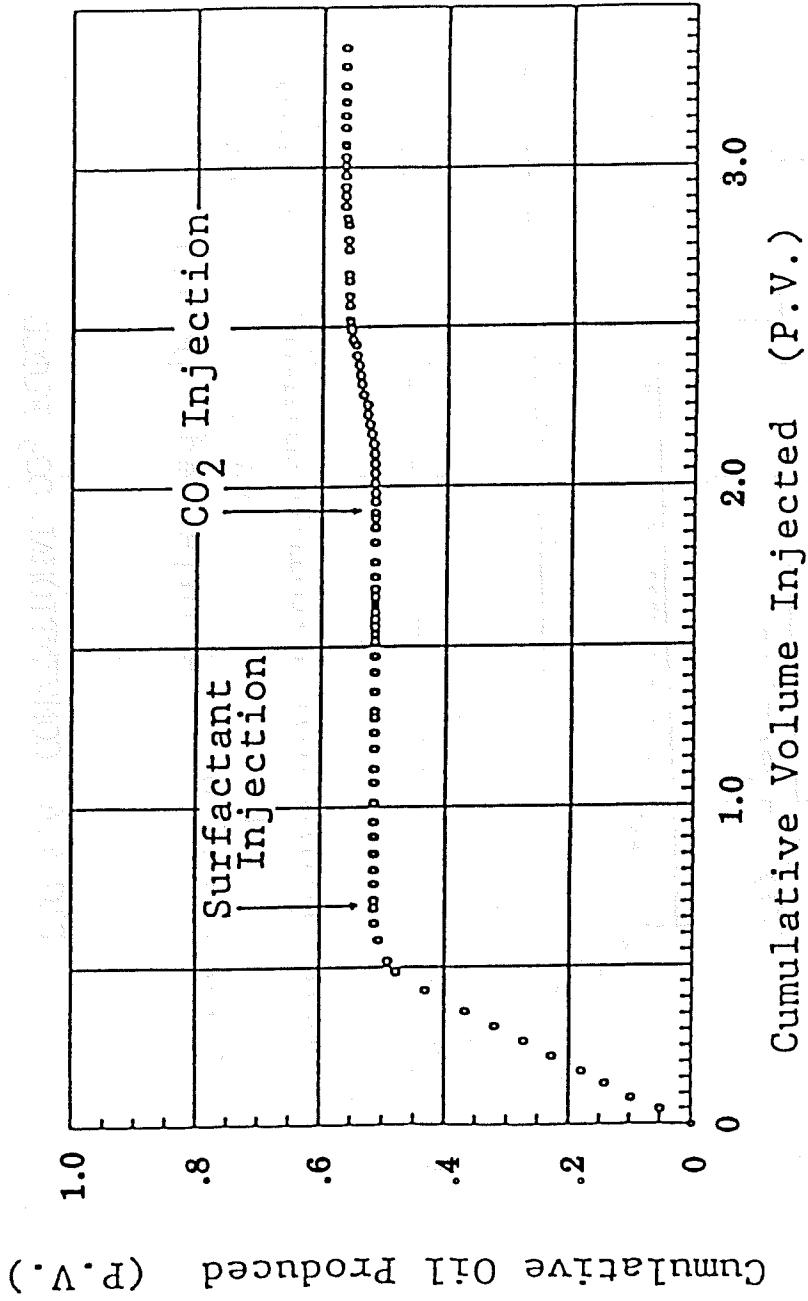


FIG 4.5: STEPANFLO 50 MOBILITY CONTROLLED CO₂ FLOOD

Supercritical CO₂ injection (T = 100°F; P = 1300 psi) was initiated after the Stepanflo-50 solution was in place. After injecting 0.6 PV of carbon dioxide, tertiary oil production commenced. Oil was produced at an approximately constant water oil ratio until 0.052 PV of tertiary oil had been produced. This is a slight decrease compared to the tertiary oil produced by carbon dioxide in the absence of a mobility control additive. The lower oil volume is not considered statistically significant.

The results obtained for mobility control additive, Pluradyne SF-27, are shown in Figure 4.6. Pluradyne SF-27 is a blend of ethoxylated alcohols having chain lengths varying between C₁₁ and C₁₅. It is superior to all other ethoxylated alcohol additives tested to date. However, additives having this general chemical structure show superior performance and several additives almost as effective are also commercially available. The waterflood performed in preparation for the Pluradyne SF-27 experiment again produced the expected 0.5 PV of oil. 1.3 PV of brine containing Pluradyne SF-27 was injected at 2.0 psi/ft pressure to prepare the model for the subsequent tertiary CO₂ flood. Tertiary oil production was delayed until 0.5 PV of carbon dioxide (T = 100°F; P = 1300 psi) had been injected. This indicates a more efficient displacement of residual oil than was observed for either the conventional CO₂ flood or the experiment performed using Stepanflo-50. Oil recovery was slightly more erratic than previously observed but culminated in an ultimate recovery of 0.07 PV incremental oil, 30 percent greater than that obtained in a conventional CO₂ flood. The lower water-oil ratio indicated a more effective banking of oil. Also the higher cumulative recovery indicates the superiority of Pluradyne SF-27 for mobility control of carbon dioxide.

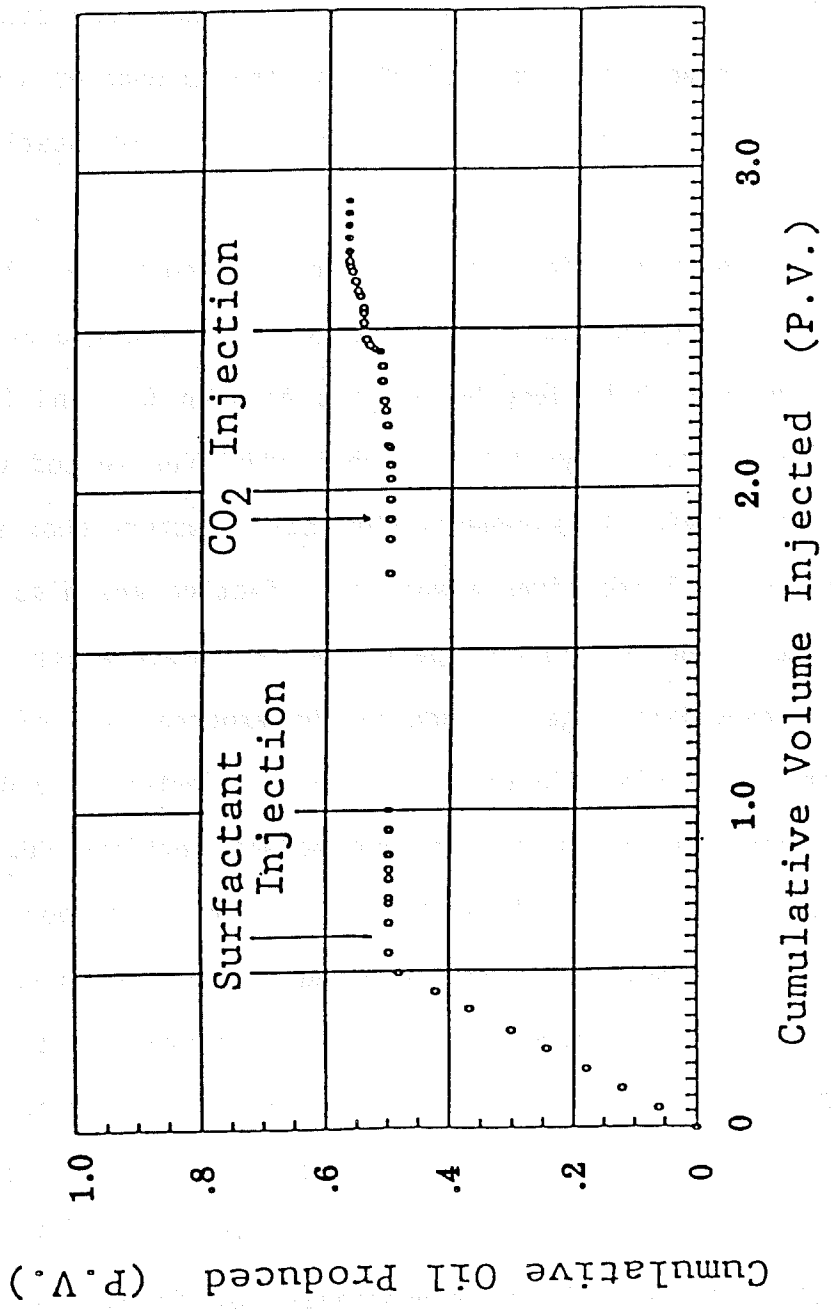


FIG 4.6: PLURADYNE SF-27 MOBILITY CONTROLLED CO₂ FLOOD

The most dramatic improvement in tertiary oil recovery was obtained using Exxon's LD 776-52. This is a synthetic sulfonate structure whose performance in brine is only average. Screening tests conducted in tap water containing very little calcium ion indicated that its potential for mobility reduction of gas flow in oil reservoirs flooded with fresh water was significantly higher than any additive previously investigated. To corroborate the superiority suggested by the dynamic screening tests, an experiment using LD 776-52 dissolved in tap water was conducted using the same model and technique previously used for miscible displacement studies in the presence of brine.

As shown in Figure 4.7, the waterflood produced about the same amount of primary plus secondary oil as observed in the other three experiments, 0.54 PV. The water phase was then carefully replaced with surfactant solution at a pressure drop of 2 psi/ft. Carbon dioxide injection was initiated and tertiary oil production did not occur until after 0.8 PV of supercritical carbon dioxide had been injected ($T = 100^{\circ}\text{F}$; $P = 1400$ psi). Enhanced oil production continued at a low water-oil ratio until 14 percent PV additional oil had been produced and residual oil saturation had been reduced to zero. This amount of tertiary oil represents almost a three-fold increase over the average obtained in the conventional CO_2 floods. It is the strongest experimental corroboration of the feasibility of CO_2 mobility control. It also indicates that it may be possible to tailor molecular structures to obtain even more potent additives for use in brine.

These results essentially complete the work task relative to mobility control of carbon dioxide for miscible displacement of oil. The above experiments were conducted using octane as the oil phase to

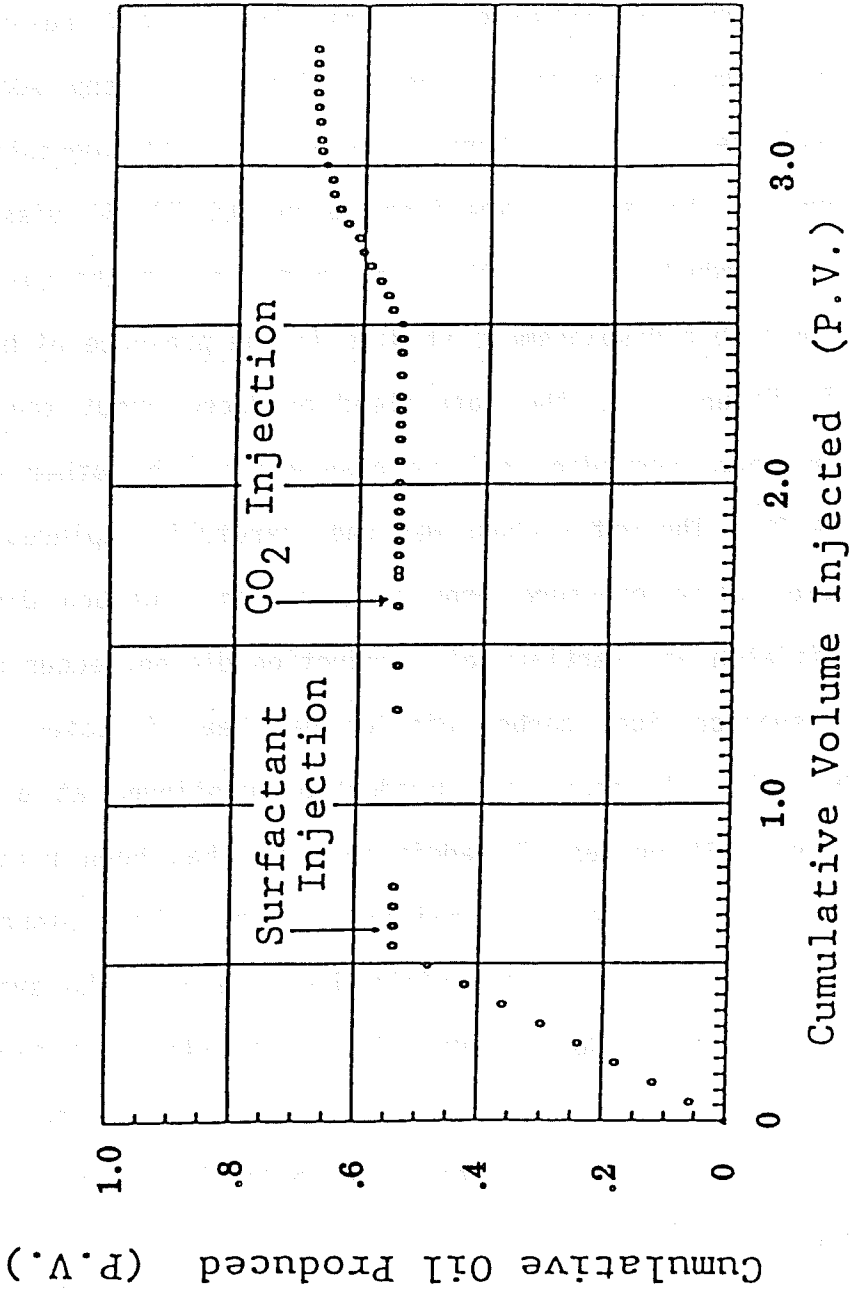


FIG 4.7: EXXON LD776-52 MOBILITY CONTROLLED CO₂ FLOOD

ensure that miscibility was obtained. The use of octane was adopted after queries of petroleum operators failed to identify an oil miscible with carbon dioxide at or below the 1500 psig pressure limitation of the experimental apparatus. The effort to find an oil, miscible with carbon dioxide within the operating limits of the equipment, will be continued and additional experiments performed if an oil from a candidate CO₂ flood reservoir is identified.

4.5 Conclusions

Each of the additives tested significantly improve the tertiary oil recoverable by carbon dioxide miscible displacement process. The feasibility of utilizing mobility control additives in the miscible process appears good with one possible exception. One cannot lower the mobility of carbon dioxide without incurring additional pressure drop in the reservoir. There are many candidate fields where the properties of the oil, coupled with the depth and temperature of the reservoir, make miscibility difficult to obtain. For these fields, any additional pressure drop, induced by a mobility control additive, could reduce the carbon dioxide pressure below the level required to achieve miscible displacement. In so doing, the additive could conceivably act to decrease oil recovery rather than increase it.

While it is easy to speculate on such an occurrence, the actual benefit or loss is most difficult to calculate. The quantitative evaluation of the effect of mobility control in a particular reservoir is best handled by computer simulation. With appropriate software, oil displacement efficiency as function of reservoir pressure, influenced by mobility control, can be mapped to predict oil displacement at

each point in the reservoir. The three dimensional nature of such simulators also can account for the improved conformance that will inevitably occur and contribute to the overall effect of mobility control on tertiary oil production. For floods below the miscibility pressure and those floods conducted well above the miscibility pressure, the use of mobility control additives should generate no adverse pressure effect and have a high potential for commercial success.

SECTION FIVE

CONCLUSIONS AND RECOMMENDATIONS

5.1 Research Summary

Commercially available surfactants, representing four classes of chemical structures, were shown to be effective in enhancing tertiary oil recovery through CO₂ mobility control. Structures having the highest potential for improving tertiary oil recovery are:

<u>TYPE</u>	<u>COMMENTS</u>
a. Ethoxylated alcohols	Cloud point may eliminate high temperature applications
b. Ethylene oxide-propylene oxide co-polymer surfactants	Cloud point may eliminate high temperature applications
c. Sulfate esters of ethoxylated alcohols (C ₉ -C ₁₆)	Hydrolytic breakdown limits application to low temperature reservoirs
d. Synthetic sulfonated surfactants	Perform best in fresh injection water and high temperature reservoirs.

The miscibility of light oils with carbon dioxide depends on the two phases achieving near equilibrium conditions in a reasonable period of time. The presence of mobility lowering surfactants at the interface was shown to have a negligible effect on the miscible interaction between carbon dioxide and n-octane. Each of three additives tested produced a measurable increase in the amount of tertiary oil displaced under miscible conditions.

The performance of all sulfonate additives tested was adversely affected by brine salinity, especially calcium ions. However, performance of a few additives of this type in fresh water, particularly at temperatures above 150°F, was so outstanding that consideration should

be given to utilizing appropriate sulfonates in fresh water to achieve good mobility control, especially in higher temperature reservoirs. The results of the miscible displacement of n-octane using Exxon's synthetic sulfonate, LD 776-52, indicate that the improvement in oil recovery could justify the added cost of fresh water or softened brine for the aqueous phase used to place the mobility additives in the reservoir.

5.2 Process Status

The feasibility of utilizing mobility control additives to enhance the recovery of tertiary oil with carbon dioxide appears good. Commercially available additives have been identified which are cost effective and compatible with a wide range of crude oils and reservoir environments. The data are conclusive that the presence of mobility control additives in no way adversely affects the dissolution of carbon dioxide into crude nor the efficiency of the the miscible displacement process.

In view of the additional pressure drop created by the presence of the mobility control additives, the process may not be applicable to very low permeability reservoirs where the added pressure drop might negate the possibility of achieving miscible pressure. The bulk of these reservoirs would be shallow, less than 5,000 feet, and contain crude oil in an intermediate gravity range, 30-38° API. Deeper reservoirs containing higher gravity oils would appear to be good candidates for initial field tests of the mobility control process.

A second class of oil reservoirs that should be prime candidates for early field tests are those with high permeabilities and high

saturations (above 50%) of low gravity crudes. Oil recovery in these reservoirs is enhanced by the immiscible CO₂ process. Incremental oil recovery due to mobility control is anticipated to be a maximum in those reservoirs containing low gravity crudes. An increase in incremental oil recovery of 39% was obtained in laboratory experiments involving displacement of a 14° API crude oil. An even greater increase in oil recovery would be anticipated in a field application where mobility control can assist in improving vertical and areal conformance problems known to exist in conventional CO₂ flooding operations.

BIBLIOGRAPHY

1. Albrecht, R. A. and Marsden, S. S. "Foams as Blocking Agents in Porous Media." Soc. Pet. Eng. J. 10, (1970), 51-55.
2. Batra, V. K. and Holm, L. W. "Model Study as a Sealant for Leaks in Gas Storage Reservoirs." Soc. Pet. Eng. J. 10, (1970), 9.
3. Beeson, D. M. and Ortloff, G. D. "Laboratory Investigation of the H₂O-Driven CO₂ Process for Oil Recovery." J. Pet. Tech. (April 1959), 63-66.
4. Bernard, G. G. "Effect of Foam on Recovery of Oil by Gas-Drive." Prod. Monthly (January 1963), Vol. 27. No. 1, 18-21.
5. Bernard, G. G. and Holm, L. W. "Effect of Foam on Permeability of Porous Media to Gas." Soc. Pet. Eng. J. (September 1964), 267-274.
6. Bernard, G. G. and Holm, L. W. "Model Study of Foam as a Sealant for Leaks in Gas Storage Reservoirs." Soc. Pet. Eng. J. 10, (1970), 9-16.
7. Bernard, G. G., Holm, L. W. and Jacobs, W. L. "Effect of Foam on Trapped Gas Saturation and on Permeability of Porous Media to H₂O." Soc. Pet. Eng. J. (December 1965), 295-300.
8. Bird, R. B., et al., Transport Phenomena, Wiley, 1960.
9. Blauer, R. E., et al., Determination of Laminar, Turbulent, and Transitional Foam Flow Losses in Pipes, SPE 4885, presented at SPE 44th Annual California Regional Meeting, San Francisco, April 4-5, 1974.
10. Bond, D. C. and Bernard, G. G. "Rheology of Foams in Porous Media." Paper presented at SPE-AIChE Joint Symposium, AIChE 58th Annual Meeting, Dallas, TX (February 1966), 7-10.
11. Brown, A. G., Thuman, W. C. and McBain, J. W. "The Surface Viscosity of Detergent Solutions as a Factor in Foam Stability." J. Colloid. Sci. 8, (1953), 491-507.
12. Chatenever, Alfred and Inora, Whit, K. and Kyte, John R. "Microscopic Observation of Solution Gas-Drive Behavior." Journal of Pet. Tech. (August 1961), 806-816.
13. "CO₂ Grows as Recovery Tool." Oil & Gas J. (August 7, 1972), 22.
14. Craig, F. F. and Lummus, J. L. "Oil Recovery by Foam Drive." U.S. Patent (1965) 3,185,634.

15. Crawford, H. R., Neill, G. H., Buck, B. J., and Crawford, P. B. "CO₂-A Multipurpose Additive for Effective Well Stimulation." J. Pet. Tech. (March 1963), 237-242.
16. Crockety, D. H. "CO₂ Profile Control at Sacroc." Pet. Eng. (November 1975), 44-52.
17. David, A. and Marsden, S. S. "The Rheology of Foam." Soc. Pet. Eng. AIME, SPE No. 2544.
18. De Nevers, N. "A Calculation Method for Carbonated Water Flooding." Soc. Pet. Eng. Journal (March 1964), 9-20.
19. De Vries, A. J. "Foam Stability." Rubber Chemistry and Technology, 1957.
20. Dicharry, R. M. "Landmark CO₂ Injection Project Pacing Off At Sacroc." Pet. Engr. (December 1974), 22-25.
21. Dicharry, R. M., Perryman, T. L., and Ronquille, J. D. "Evaluation and Design of a CO₂ Miscible Flood Project-Sacroc Unit, Kelly-Snyder Field." J. Pet. Tech. (November 1973), 1309-1318.
22. Dodds, W. S., Stutzman, L. F., Sollami, B. J. "CO₂ Solubility in H₂O." Ind. & Eng. Chem. (1956), 92.
23. ERDA "Enhancement of Recovery of Oil & Gas." Progress Review #9 (January 1977).
24. Eugenev, A. E. and Turnier, V. N. "Rheological Properties of Foam in Porous Medium." Neft-I-Gaz Vol. 10 No. 12 (1967), 78-80.
25. Eydt, A. J. "Study of the Foamability of Solutions Using the Tensiolaminometric Technique." Jour. Am. Oil Chem. Soc., Vol. 45 (September 1968), 607-610.
26. Francis, A. W. "Ternary Systems of Liquid CO₂." J. Phys. Chem. Vol. 58 (December 1954), 1099-1114.
27. Fried, A. N. "The Foam-Drive Process For Increasing the Recovery of Oil." R. I. 5866, USBM (1961).
28. Gooktekin, A. "Experimental Studies on the Production of Foams in Porous Media with a View to Increasing the Recovery of Oil from a Reservoir." Erdoel-Erdgas-Z. Vol. 84, No. 6 (1968), 208-226.
29. Henderson, L. E. "The Use of Numerical Simulation to Design a CO₂ Miscible Displacement Project." J. Pet. Tech. (December 1974), 1327-1334.
30. Herschel, W. H., and R. Bulkley, Proceedings, ASTM, 26, Part II, 621-633, (1926).

31. Hoffer, M. S. and Rubin, E. "Flow Regimes of Stable Foams." Ind. Eng. Chem. Fundam. Vol. 8, No. 3 (August 1969), 438-489.
32. Holbrook, S. T., et al. "Rheology of Mobility Control Foams." Paper SPE/DOE 9809 presented at the 1981 SPE/DOE Second Joint Symposium on EOR, Tulsa, April 5-8, 1981.
33. Holm, L. W. "A Comparison of Propane and CO₂ Solvent Flooding Processes." AICHE Journal Vol. 7, No. 2 (June, 1961), 179-184.
34. Holm, L. W. "CO₂ Requirements in CO₂ Slug and Carbonated H₂O Oil Recovery Processes." Prod. Monthly (September 1963), 6-8, 26-28.
35. Holm, L. W. "CO₂ Solvent Flooding for Increased Oil Recovery." Pet. Trans. AIME Vol. 216 (1959), 225-231.
36. Holm, L. W. "Foam Injection Test in the Siggins Field, Illinois." J. Pet. Tech. Vol. 22 (1970), 1449-1506.
37. Holm, L. W. "Model Study of Foam as a Sealant for Leaks in Gas Storage Reservoirs." Soc. Pet. Engrs. Jour. Vol. 10 (1970), 9.
38. Holm, L. W. "Status of CO₂ and Hydrocarbon Miscible Oil Recovery Methods." J. Pet. Tech. (January 1976), 76-84.
39. Holm, L. W. "The Mechanism of Gas and Liquid Flow Through Porous Media in the Presence of Foam." Soc. Pet. Eng. J. (December 1968), 359-369.
40. Holm, L. W. and Josendal, V. A. "Mechanisms of Oil Displacement by CO₂." J. Pet. Tech. (December 1974), 1427-1438.
41. Holm, L. W. and O'Brian, L. J. "CO₂ Test at the Mead-Strawn Field." J. Pet. Tech. (1971), 431-442.
42. Huang, E. T. S., and Tracht, J. H. "The Displacement of Residual Oil by CO₂." Paper SPE 4735 Presented at the SPE-AIME 3rd Symposium on Improved Oil Recovery, Tulsa (April 22-24, 1974).
43. Jacob, W. M., Woodcock, K. E. and Grove, C. S. "Theoretical Investigation of Foam Drainage." Ind. & Chem. Vol. 48, No. 11 (November 1956), 2046-2051.
44. Kanda, M., Schechter, R. S. "On the Mechanism of Foam Formation in Porous Media." Paper SPE 6200, Society of Petroleum Engineers of AIME, 5200 North Central Expressway, Dallas, TX. 75206 1976.
45. Kohler, N. and G. Chauveteau. "Polysaccharide Plugging Behavior in Porous Media: Preferential Use of Fermentation Broth." Paper SPE 7425 presented at SPE 53rd Annual Fall Meeting, Houston, October 1-4, 1978.

46. Lacy, J. W., Faris, J. E. and Brinkman, F. H. "Effect of Bank Size on Oil Recovery in High Pressure Gas-Driven LPG-Bank Process." Journal of Pet. Tech. (August 1961), 806-816.
47. Marsden, S. S. and Khan, S. A. "The Flow of Foam through Short Porous Media and Apparent Viscosity Measurements." Soc. Pet. Eng. J. (March 1966), 17-25.
48. Marsden, S. S., Jr., Earligh, J. J. P., and Albrecht, R. A. "Use of Foam in Petroleum Operations." Paper presented at Seventh World Pet. Cong., Mexico City (April 2-7, 1967).
49. Mast, R. F. "Microscopic Behavior of Foam in Porous Media." Paper SPE 3997, Society of Petroleum Engineers of AIME, 6200 North Central Expressway, Dallas, TX 75206 1972.
50. Menzie, D. E., and Nielson, R. F. "A Study of the Vaporization of Crude Oil by CO₂ Repressurization." J. Pet. Tech. (November 1963), 1247-1252.
51. Metzner, A. B. "Flow of Non-Newtonian Fluids." Handbook of Fluid Dynamics, McGraw Hill, 1st Edition, 1961.
52. Michels, A., Botzen, A., and Schuurman, W. "The Viscosity of CO₂ Between 0°C and 75°C and at Pressures up to 2000 Atm." Physica XXIII (1957), 95-102.
53. Mies, G. D., Shedlousky, L., and Ross, J. "Foam Drainage." Jour. Phys. Chem. Vol. 49 (1949), 93-107.
54. Minnsieux, L. "Oil Displacement by Foams in Relation to Their Physical Properties in Porous Media." J. Pet. Tech. (January 1974), 100-107.
55. Oh, S. G. and Slattery, J. C. "Interfacial Tension Required for Significant Displacement of Residual Oil." Soc. Pet. Eng. J. Vol. 19 (1979).
56. Patton, J. T. "Enhanced Oil Recovery by Carbon Dioxide Flooding," Energy Communications (January 1978), 1-24.
57. Patton, J. T. and W. E. Holman. "Removal of Water from Boreholes," U.S. Patent 3,251,417, i. May 17, 1966.
58. Rathmell, J. J., Stalkup, F. I., and Hassinger, R. C. "A Laboratory Investigation of Miscible Displacement by CO₂." Paper SPE 3483 presented at the SPE-AIME 46th Annual Fall Meeting, New Orleans, October 3-6, 1971.
59. Raza, S. H. "Foam in Porous Media: Characteristics and Potential Applications." Soc. Pet. Engr. J. (December 1970), 328-336.

60. Raza, S. H. "Plugging Formations with Foam." U.S. Patent (January 27, 1970) 3,491,832.
61. Raza, S. H. and Marsden, S. S. "The Streaming Potential and the Rheology of Foam." Soc. Pet. Eng. J. (December 1967), 359-368.
62. Rogers, W. F. "Lab Apparatus for Studying Oil Well Subsurface Corrosion." Corrosion, Vol. 9 No. 25 (January 1953).
63. Rosen, M. J. and Solash, J. "Factors Affecting Initial Foam Height in the Ross-Miles Foam Test." Jour. Am. Oil Chem. Soc. (August 1969), 399-402.
64. Ross, S. "Bubbles and Foam: New General Law." Ind. & Eng. Chem., Vol. 61 No. 10 (October 1969), 49-57.
65. Scheideger, A. E. The Physics of Flow Through Porous Media, McMillan Company, 2 ed. New York, 1960.
66. Scott, J. O. and Forrester, C. E. "Performance of Domes Unit Carbonated Waterflood-First Stage." J. Pet. Tech. (September 1965), 1379-1384.
67. Shah, D. O. and Syslesui, C. A. "Molecular Interactions in Monolayers: Molecular Association and Foam Stability of Fatty Acids and Alcohols." Jour. A. Oil. Chem. Soc. (December 1969), 645-648.
68. "Shell Starts Miscible CO₂ Pilot in Mississippi's Little Creek Field." Oil & Gas J. (September 2, 1974), 52-53.
69. Shelton, J. L. and Schnieder, F. N. "The Effect of H₂O Injection on Miscible Flooding Methods Using Hydrocarbons and CO₂" Soc. Pet. Eng. J. (June 1975), 217-226.
70. Shelton, J. L. and Yarborough, L. "Multiple Phase Behavior in Porous Media During CO₂ or Rich-Gas Flooding." J. Pet. Tech. (September 1977), 1171-1178.
71. Shih, F. S. and Lemlich, R. "Continuous Foam Drainage and Overflow." Ind. Eng. Chem. Fundam. Vol. 10 No. 2 (1971), 2547-259.
72. Sibree, T. O. "The Viscosity of Froth." Trans. Farad. Soc. Volume 30 (1934), 325-331.
73. Simon, R. and Graue, D. J. "Generalized Correlations for Predicting Solubility, Swelling, and Viscosity Behavior of CO₂ - Crude Oil Systems." J. Pet. Tech. (January 1965), 102-106.
74. Slattery, J. C. "Interfacial Effects in the Displacement of Residual Oil by Foam." AIChE Journal. Vol. 25 No. 2 (March 1979), 283-289.

75. Smith, R. L. "Sacroc Initiates Landmark CO₂ Injection Project." Pet. Eng. (December 1971), 43-47.
76. Snyder, R. E. "Shell Starts CO₂ Injection Project in West Texas." World Oil (September 1972), 75-76.
77. Spangler, W. G. "Dynamic Foam Test." Jour. Am. Oil. Chem. Soc. Vol. 41 (April 1964), 300-306.
78. Stright, D. H., Aziz, K., Settari, A., and Starratt, F. E. "CO₂ Injection into Bottom-Water Undersaturated Viscous Oil Reservoirs." J. Pet. Tech. (October 1977), 1248-1258.
79. Van Meures, P. "The Use of Transparent Three-Dimensional Models for Study of the Mechanisms of Flow Processes in Oil Recoveries." Trans. AIME 210 (1957), 205-301.
80. Van Waxer, J. R., et al., Viscosity and Flow Measurement - A Laboratory Handbook of Rheology, Interscience Publishers, 1963.
81. Warner, H. R., Jr. "An Evaluation of Miscible CO₂ Flooding in Waterflooded Sandstone Reservoirs." J. Pet. Tech. (October 1977), 1339-1347.
82. White, R. W. "Oil Recovery by CO₂: Past and Future." Pet. Engr. (December 1971), 58-59.
83. Whorton, L. P. Brownscombe, E. R. and Dyes, A. B. "Method for Producing Oil by Means of CO₂." U.S. Patent (December 30, 1952) 2,623,596
84. Wilson, Keith. "Enhanced Recovery Inert Gas Processes Compared." Oil & Gas J. (July 31, 1978) 76.
85. Bernard, G. G., Holm, L. W. and Harvey, C. P. "Use of Surfactant to Reduce CO₂ Mobility in Oil Displacement." Soc. Pet. Eng. J. (August 1980), 281-292.
86. Buckley, S. E. and Leverett, M. C. "Mechanisms of Fluid Displacement in Soils." Trans. AIME 142, (1942) 152.
87. Johnson, Bossler & Nauman, Trans. AIME 216, (1959) 370.
88. Patton, J. T. "Enhanced Oil Recovery by CO₂ Foam Flooding." Final Report, U.S. Doe DE8200905 (April 1982).
89. Collines, R. E. Flow of Fluids Through Porous Media, The Petroleum Publishing Co., Tulsa (1976).
90. Kestin, J., Whitelaw, J. H. and Zien, T. F., Physica 30, 161 (1964).
91. Michels, A., Bolzen, A., and Schuurman, Physica 20, 1141 (1941).
92. Perry, R. H. and Chilton, C. H. "Chemical Engineers' Handbook," 3rd ed., McGraw-Hill, New York (1973).

93. Welge, H. J. "A Simplified Method for Computing Oil Recovery by Gas or Water Drive," Trans. AIME 195, 91 (1952).

94-100. Reserved for future references.

PATENTS & THESES

101. Bernard, G. G.: "Foam Drive Oil Recovery Process," U.S. Patent No. 3,529,668 (1970).
102. Bernard, G. G. and Bond, D. C.: "Forming Foam Under Reservoir Conditions in Petroleum Recovery Process", U.S. Patent No. 3,318,379 (1967).
103. Bernard, G. G. and Bond, D. C.: "Secondary Recovery Method," U.S. Patent No. 3,369,601 (1968).
104. Bernard, G. G. and Holm, L. W.: "Method for Recovering Oil from Subterranean Formations," U.S. Patent No. 3,342,256 (1967).
105. Bernard, G. G. and Rai, C.: "Method of Secondary Recovery Employing Successive Foam Drives of Different Ionic Characteristics," U.S. Patent No. 3,323,588 (1967).
106. Bond, D. C. and Holbrook, O. C.: "Gas Drive Oil Recovery Process," U.S. Patent No. 2,866,507 (1958).
107. Craig, F. F. and Lummus, J. L. "Oil Recovery by Foam Drive." U. S. Patent (1965), 3, 185, 634.
108. Deming, J. R.: "Fundamental Properties of Foams and Their Effects on the Efficiency of the Foam Drive Process," M.S. Thesis, The Pennsylvania State U. (1964).
109. Holm, L. R. W.: "Secondary Recovery Process Using Gas-Liquid Drive Fluids," U.S. Patent No. 3,177,939 (1965).
110. Holman, W. E. and Patton, J. T.: "Removal of Water Boreholes," U.S. Patent No. 3,251,417 (1966).
111. Patton, J. T., "Modified Heteropolysaccharides," U.S. Patent 3,729,460, i. May 24, 1973.
112. Raza, S. H. "Plugging Formations with Foam." U. S. Patent #3,491,832 (January 27, 1970).
113. Whorton, R. W. "Oil Recovery by CO₂: Past and Future." Pet. Engr. (December 1971), 58-59.

APPENDIX A

APPENDIX A

APPENDIX A

Surfactant Chemical Structures

<u>Surfactant</u>	<u>Chemical composition</u>	<u>Code</u>
<u>AMOCO</u>		
Cosurfactant 120	6-mole adduct of ethoxylated hexyl alcohol + distribution of higher and lower adducts	1:3
Cosurfactant 122	6-mole adduct of ethoxylated amyl alcohol + distribution of higher and lower adducts	1:4
Sulfonate 151	Sodium salt of a polybutene sulfonate with a broad equivalent wt. distribution with an average of 400-420	1:1
Sulfonate 152	Sulfonated specially treated vacuum-gas oil with a broad equivalent wt. distribution of 400-420 average	1:2
<u>Armak</u>		
Aromox C/12	bis (2-hydroxyethyl) cocoamine oxide and aqueous isopropanol	2:2
Aromox T/12	bis (2-hydroxyethyl) tallowamine oxide and aqueous isopropanol	2:1
Aromox DM16	dimethylhexadecylamine oxide and aqueous isopropanol	2:3
Aromox DMC	dimethylcocoamine oxide and aqueous isopropanol	2:4
Armeen Z	N-coco-betaaminobutyric acid	2:7
Ethomeen 18/25	$R-N \begin{matrix} \text{---} (\text{CH}_2\text{CH}_2\text{O})_x \text{H} \\ \text{---} (\text{CH}_2\text{CH}_2\text{O})_y \text{H} \end{matrix}$ where $x+y=15$	2:5
Ethomeen 18/60	and $R = \text{CH}_3(\text{CH}_2)_{16} \begin{matrix} \text{---} \text{C} \text{---} \text{O} \\ \text{---} \text{OH} \end{matrix}$ The same ethoxylate as above where $x+y=50$ and $R = \text{CH}_3(\text{CH}_2)_{16} \begin{matrix} \text{---} \text{C} \text{---} \text{O} \\ \text{---} \text{OH} \end{matrix}$	2:6
<u>BASF Wyandotte</u>		
ES-179	unknown	3:23
Klearfac AA 270	phosphate ester	3:14
Klearfac AA 420	phosphate ester	3:15
Pluronic F68	$\text{HO}(\text{CH}_2\text{CH}_2\text{O})_a \underset{\text{CH}_3}{\text{C}}(\text{CH}_2\text{CH}_2\text{O})_b (\text{CH}_2\text{CH}_2\text{O})_c \text{H}$	3:1
	Molecular wt. = 8,350 80% poly(oxyethylene)	

APPENDIX A

<u>Surfactant</u>	<u>Chemical composition</u>	<u>Code</u>
<u>BASF Wyandotte</u>		
Pluronic F87	$\text{HO}(\text{CH}_2\text{CH}_2\text{O})_a(\text{CH}_2\text{CH}_2\text{O})_b(\text{CH}_2\text{CH}_2\text{O})_c\text{H}$ CH_3	3:2
	Molecular wt. = 7,700	
	70% poly(oxyethylene)	
Pluronic F108	" , 14,000, 80%	3:3
Pluronic L62	" , 2,500, 20%	3:4
Pluronic L64	" , 2,900, 40%	3:5
Pluronic P85	" , 4,600, 50%	3:6
Pluronic P103	" , 4,950, 30%	3:7
Pluronic P104	" , 5,850, 40%	3:8
Pluronic P105	" , 6,500, 50%	3:9
Pluronic 25R2	" , 3,120, 20%	3:10
Pluronic 25R4	" , 3,800, 40%	3:11
Pluronic 25R5	" , 4,500, 50%	3:12
Pluronic 25R8	" , 9,000, 80%	3:13
Tetronic 904	$\text{H}(\text{C}_2\text{H}_4\text{O})_y(\text{C}_3\text{H}_6\text{O})_x\text{N}(\text{C}_3\text{H}_6\text{O})_x(\text{C}_2\text{H}_4\text{O})_y\text{H}$ $\text{H}(\text{C}_2\text{H}_4\text{O})_y(\text{C}_3\text{H}_6\text{O})_x\text{N}(\text{C}_3\text{H}_6\text{O})_x(\text{C}_2\text{H}_4\text{O})_y\text{H}$	3:18
	Molecular wt. = 7,500	
	40% poly(oxyethylene)	
Tetronic 908	" , 27,000, 80%	3:19
Tetronic 1501	" , 7,900, 10%	3:20
Tetronic 1504	" , 12,500, 40%	3:21
Tetronic 1508	" , 27,000, 80%	3:22
Tetronic 50R4	$\text{H}(\text{C}_3\text{H}_6\text{O})_y(\text{C}_2\text{H}_4\text{O})_x\text{N}(\text{C}_2\text{H}_4\text{O})_x(\text{C}_3\text{H}_6\text{O})_y\text{H}$ $\text{H}(\text{C}_3\text{H}_6\text{O})_y(\text{C}_2\text{H}_4\text{O})_x\text{N}(\text{C}_2\text{H}_4\text{O})_x(\text{C}_3\text{H}_6\text{O})_y\text{H}$	3:16
	Molecular wt. = 50,000	
	40% poly(oxyethylene)	
Tetronic 150R4	" 150,000, 40%	3:17
<u>Conoco</u>		
Alfonic 610-50	$\text{CH}_3(\text{CH}_2)_x\text{CH}_2(\text{OCH}_2\text{CH}_2)_n\text{OH}$	5:1
	where x= 4-8, n= 3	
Alfonic 1012-40	" , x= 8-10, n= 2.5	5:2
Alfonic 1012-60	" , x= 8-10, n= 5.7	5:3
Alfonic 1216-22	" , x= 10-14, n= 1.2	5:4
Alfonic 1412-40	" , x= 10-12, n= 3	5:5
Alfonic 1412-60	" , x= 10-12, n= 7	5:6
Alfonic 1218-70	" , x= 10-16, n= 10.7	5:7

APPENDIX A

<u>Surfactant</u>	<u>Chemical composition</u>	<u>Code</u>
<u>Dow</u>		
Dowfax 2A1	sodium dodecyl diphenyl ether disulfonate and sodium didodecyl diphenyl ether disulfonate	6:1
Dowfax 3B2	sodium decyl diphenyl ether disulfonate and sodium didecyl diphenyl ether disulfonate	6:2
XD-8390	sodium hexadecyl diphenyl ether disulfonate	6:3
<u>Exxon</u>		
Corexit 8534	inorganic salt of oxyalkylated sulfated alcohol	7:1
<u>GAF</u>		
Alipal CD-128	nonadecyldiethoxy ammonium sulfate	8:1
Alipal CO-436	nonylphenoxypolyethoxyethanol	8:2
<u>Mona, Ind.</u>		
Monamid 150AD	$ \begin{array}{c} \text{O} \quad \text{H} \\ \parallel \quad \\ \text{R}_2 - \text{C} - \text{N} - \text{CH}_2 - \text{CHOH} \\ \quad \quad \quad \\ \quad \quad \quad \text{R}_1 \end{array} \quad \& \quad \begin{array}{c} \text{O} \quad \text{CH}_2\text{CH}_2\text{OH} \\ \parallel \quad \\ \text{R}_2 - \text{C} - \text{N} - \text{CH}_2\text{CH}_2\text{OH} \end{array} $	9:1
	where $\text{R}_1 = \text{H}$ or CH_3 , $\text{R}_2 =$ coconut fatty acid	
<u>Nalco</u>		
Adofoam BF-1	alcohol ether sulfate ammonium salt	10:1
Visco 1111	ethylene oxide adducts of alkylated phenols, alcohols and fatty acids	10:2
Visco 1152	3-alkoxy-2-hydroxy-N-propyl trimethyl ammonium chloride	10:3
<u>Petrochem</u>		
Norwet IP Powder	2,5-diisopropyl-8-methyl naphthalene sodium sulfonate	11:1
Petro BAF Powder	2-dodecyl-8-methyl naphthalene sodium sulfonate (25%), and 8-methyl naphthalene sodium sulfonate (75%)	11:3
Petro BAF Liquid	Same as Petro BAF Powder except in 50% aqueous solution	11:2
Petro P Powder	2-nonyl-8-methyl naphthalene sodium sulfonate (30%), and 8-methyl naphthalene sodium sulfonate (70%)	11:5
Petro P Liquid	Same as Petro P Powder except in 50% aqueous solution	11:4
Udet 950	2-dodecyl-8-methyl naphthalene sodium sulfonate (50%), and 8-methyl naphthalene sodium sulfonate (50%)	11:6

<u>Surfactant</u>	<u>Chemical composition</u>	<u>Code</u>
<u>Proctor & Gamble</u>		
Amide #27	coconut monoethanolamide	12:1
CO-1214N	fatty alcohol; 67% C ₁₂ , 6% C ₁₆	12:2
Equex AEM	ammonium lauryl ether sulfate (38%), alkanolamide (9%)	12:3
<u>Rohm & Haas</u>		
Triton X-100	octylphenyl nonylethoxy ethanol	13:1
Triton X-165	octylphenyl hexadecylethoxy ethanol	13:2
Triton X-200	sodium alkylaryl polyether sulfonate	13:3
Triton X-301	sodium alkylaryl ether sulfate	13:4
Triton X-405	octylphenyl tetracontylethoxy ethanol	13:5
<u>Shell</u>		
Neodol 23-3	C ₁₂ -C ₁₃ linear, primary alcohol propylethoxylate	14:1
Neodol 25-7	C ₁₂ -C ₁₅ linear, primary alcohol heptylethoxylate	14:2
Neodol 25-12	C ₁₂ -C ₁₅ linear, primary alcohol dodecylethoxylate	14:3
Neodol 91-2.5	C ₉ -C ₁₁ linear, primary alcohol diethoxylate	14:4
Neodol 91-8	C ₉ -C ₁₁ linear, primary alcohol octylethoxylate	14:5
<u>Union Carbide</u>		
Tergitol TMN-6	trimethyl nonyl polyethylene glycol ether	4:1
Tergitol 15-S-40	polyethylene glycol ether of linear alcohol	4:2
<u>Witco</u>		
Emcol CC37-18	unknown	15:1
Emcol CMCD	amphoterics derived from coconut oil	15:2
Sulframin AOS	alpha olefin sulfonate consisting primarily of 14-16 carbon chain dist- ribution	15:3
Sulframin 1250	linear alkylaryl sodium sulfonate	15:4
TRS X-107,203	petroleum sodium sulfonates	15:5, 15:6
301,401		15:7, 15:8
501,601		15:9, 15:10
Witcamide 5195	lauric diethanolamide	15:11
Witcolate 1247-H	unknown	15:12
Witcolate 1259	unknown	15:13
Witcolate 1276	alcohol ether sulfate	15:14

A P P E N D I X B

Appendix B

Blender Foam Test

Objective:

The objective of the foam test is to measure the foamability of surfactant solutions and the stability of the resultant foams in a manner which yields accurate and reproducible results. Foamability is the initial height of the foam after generating it with a blender, and stability is the resistance of the foam to decay.

Apparatus:

The foam is generated in a Pulsmatic 10 Osterizer blender. A three inch O. D. Plexiglass tube, at least 24 inches long, is fitted to the base of the blender and used as the container for both the blending and the measurement of foam height. The surfactant concentration is usually 0.5%, but it may be specified otherwise for particular tests.

Procedure:

1. All data including surfactant name, concentration, pH, volume used, blending speed, blending time, and foam height vs. time will be recorded in one of the EOR lab data books.
2. The surfactant solutions are prepared by weighing 1.0 g of surfactant in a bottle of approximately 110 ml volume. 100 ml of brine is then added to the bottle, and the surfactant is allowed time to dissolve before it is tested. If the solution must be agitated, time must be allowed for any foam generated from the agitation to settle before the surfactant solution can be tested.

3. Before subjecting any surfactant to the blender test, the pH of the solution is adjusted to 2.5 - 2.7. Pour the 100 ml of solution from the bottle into a beaker, add 100 ml of brine, and measure the pH of the solution. Use a magnetic stirrer to maintain a well mixed system, but keep the stirring rate low to prevent foaming. Add hydrochloric acid dropwise until the pH is within the proper range.
4. Pour the pH-adjusted solution into a blender cylinder. Allow it to run down the wall rather than falling to the bottom to prevent foam generation due to pouring.
5. Prepare a table for recording foam heights such as the one below:

TIME (min)	TOP (cm)	BOTTOM (cm)	VOLUME (ml)
---------------	-------------	----------------	----------------

The time will start at 0 and end at 20 minutes.

6. Blend at puree speed for 15 seconds. Puree speed is approximately 10,000 RPM.
7. At time = 0, when the blender blades have stopped rotating, record the heights at the foam surface and the foam liquid interface. If the interface can't be seen, record it as zero initially, but do not record any value for it again until it can be seen clearly.
8. Measure the heights of the foam surface and the foam liquid interface at two-minute intervals for a period of 20 minutes.
9. After the test, rinse the cylinder well with tap water. The absence of any foam indicates the surfactant has been rinsed out. Give the column a final rinse with Reverse Osmosis water and allow to drain well.

10. To calculate the foam volume, use the following information:

A column height of 1.3 cm is equivalent to a 50 ml volume.

Since the base of the cylinder is not uniform to the rest,

the 3.5 cm mark is equivalent to 100 ml. The foam volume

is then calculated by the formula:

$$\text{Vol} = ((\text{Top} - \text{Bottom}) \times 50) + 1.3$$

Vol is foam volume in ml

Top is height of foam surface in cm

Bottom is height of foam liquid interface in cm

In those cases where the foam liquid interface can't be seen for the initial reading (time = 0), use 3.5 as the bottom value and add 100 ml to the foam volume calculated from the above equation.